Development of a Nanoparticle Vaccine Delivery System with Polymeric Oral Adjuvants for Poultry

Jewel M. Cary

Dissertation submitted to the faculty of the
Virginia Polytechnic Institute and State University
in partial fulfillment of the requirements for the degree of

Doctor of Philosophy
in
Biomedical Engineering

Abby R. Whittington, Chair
Frank William Pierson, Co-Chair
Kevin J. Edgar
Mark Van Dyke
Yong Woo Lee

July 29th, 2019
Blacksburg, Virginia

Keywords: Nanoparticles, Poultry Medicine, Vaccine Development, Polymeric Adjuvants

Development of a Nanoparticle Vaccine Delivery System with Polymeric Oral Adjuvants for Poultry

Jewel M. Cary

ABSTRACT

Development of new vaccination technology has been hindered by a lack of new adjuvants to enable development of protective immunity using different vaccine delivery methods. A vaccine delivery system using oral adjuvants would be applicable across species for both individual and mass vaccination in both the medical and veterinary fields. We sought to create an oral nanoparticle (NP) vaccine delivery system that is easy to produce and uses polymers as oral adjuvants with killed virus. Our hypothesis was gelatin and chitosan would enhance viral uptake and stimulate immune cells to produce protective immunity. This would allow the safer killed form of each virus to be used in place of modified live (MLV) viruses and avoid undesirable side effects like immunosuppression. The research objectives were to

1. Fabricate and characterize gelatin NPs encapsulating inert materials of similar size and shape to the viruses of interest for fabrication proof-of-concept
2. Modify the NP delivery system to minimize immune cell cytoxicity for the vaccine delivery application
3. Fabricate and characterize FPV and HEV viral nanoparticles' stability, cellular uptake/infectivity, and released viruses' ability to replicate
4. Compare the abilities of the killed HEV nanovaccine, killed HEV with loose gelatin and chitosan polymers (no nanoparticle), and a live HEV commercial vaccine to induce *in vivo* seroconversion, protective immunity, and side effects during clinical and challenge studies in turkeys

We proved our hypothesis to be correct in addition to demonstrating matching the encapsulation material size to empty NP size leads to preferred encapsulated NP formulation parameters, chitosan stabilizes the NP formulation bypassing the need for cytotoxic crosslinkers, and paraformaldehyde is able to kill virus prior to vaccine formulation while still preserving virus morphology sufficiently for immune cell recognition. This development constitutes one of the first novel adjuvants discoveries in 70 years and opens the door for conversion of injectable vaccines to oral delivery across species.

Development of a Nanoparticle Vaccine Delivery System with Polymeric Oral Adjuvants for Poultry

Jewel M. Cary

GENERAL AUDIENCE ABSTRACT

Most vaccinations use needles to inject a live but weakened virus into the body, which causes a mild infection. The body learns to protect itself using this weak form of the virus, so that when the body encounters a stronger form of the same virus later on in life, the body is able to quickly kill the virus and recover from the infection. If we could package a dead virus with the right mixture, we could get the body to recognize the dead virus and learn to protect itself just as the body does with the weaker, live virus. This would avoid the mild infection and the unpleasant symptoms associated with the live virus injection and allow us to use a safer dead virus vaccine. Additionally, with the right package, we could drink our vaccines instead of using injections. Here, we tried to create a drinkable, safer dead virus packaged with gelatin and shellfish fiber in a vaccine that allows the body could recognize the dead virus and learn to protect itself similarly to the live virus vaccine. The goals of this work were to:

1. Practice putting plastic beads of similar size and shape to viruses in gelatin packages to understand how to safely package viruses in gelatin as part of making the new drinkable vaccine
2. Adjust the process of making the gelatin plastic bead packages to work well with cells in the laboratory as a second step toward making safe vaccines
3. Use the packaging process to package a dead chicken virus and a dead turkey virus separately with gelatin and shellfish fiber and measure each packaged virus
4. Test the dead packaged turkey virus vaccine with gelatin and shellfish fiber, the dead unpackaged turkey virus with loose gelatin and shellfish fiber, and a live turkey virus that is currently used as a vaccine in turkeys to see which allows the body to protect itself without causing side effects

We showed that using plastic beads of similar size to empty gelatin and shellfish fiber packages creates the preferred packaged plastic bead measurements. The shellfish fiber kept the packages intact and from falling apart, so no additional chemicals were needed. The preservative used to kill the virus worked while still keeping the virus recognizable to the body. This new packaging for vaccines is a breakthrough in vaccine development and will allow us to change injectable vaccines to drinkable vaccines in other animals and humans.

Contents

Chapter 1

Introduction

1.1 Motivation

The key factor preventing development of the next generation of vaccine technology is a lack of new oral adjuvants. New oral adjuvants would open up the field of vaccine development to include vaccines that induce mucosal immunity, which is the body's first line of defense against most pathogens. Vaccines that induce immunity at the mucosal surface instead of or in addition to systemic immunity would be more efficient at fighting off pathogens before an infection has moved further into the body[65]. Using killed viruses in vaccine formulations improves the safety of the vaccination as the virus cannot replicate and therefore cannot cause side effects like immunosuppression leading to secondary infections [66, 15]. Our goal in this research is to create a nanoparticle vaccine delivery system using gelatin and chitosan as oral adjuvants to stimulate protective immunity with killed virus. The short-range benefit of achieving the aforementioned research objectives would be to address the need in the poultry industry for safer mass vaccination delivery systems. The long-range benefit would be to advance knowledge in vaccine development, specifically in determining whether gelatin and chitosan oral adjuvants can bypass the need for modified-live viruses to induce protective immunity with oral delivery. Additionally, this work will determine whether chemical fixative can both kill virus and still preserve viral morphology for immune cell recognition of the virus in a nanovaccine formulation. This nanoparticle (NP) delivery technology has the potential for use with multiple viruses, polyvalent vaccine development, delivery of drugs or other biologics, and cross-species vaccine delivery.

The background discussed in the following sections will set the stage for the body of work outlined in the upcoming research studies. The current state of vaccine technology development will be reviewed to better

understand the need for novel adjuvants for conversion of injectable vaccines to oral vaccines. The reasoning behind the choice to pursue the fowlpox and hemorrhagic enteritis viruses as first approach vaccines will be enumerated. Safety concerns about both viruses will be discussed as well as the current literature research on both vaccine formulations. Finally, we will delve into the proposed approach, the choice to pursue polymeric oral adjuvants, and the double desolvation technique for nanovaccine formulation.

1.2 Current State of Vaccine Technology Development

Vaccine delivery systems are typically tailored to specific diseases and species in an all-inclusive package that includes the specific antigen, adjuvant, delivery method, and species of interest. Currently, many commercial vaccines are injectable and use alum salts as an adjuvant to induce systemic immunity. Alum salts are the most widely used vaccine adjuvant and have been in use for more than 70 years. However, this adjuvant induces a strong inflammatory reaction and is unsuitable for alternative vaccine delivery methods [15, 37]. Improved vaccines would induce immunity at the mucosal surface to allow the body to fight off the initial invasion and prevent the infection spreading into the body [15]. To create the next generation of vaccines, new adjuvants are needed.

Current vaccine development approaches are hindered by a lack of efficacious, safe, minimal side effect adjuvants to aid recombinant, synthetic, component, or whole killed antigen materials in inducing a sufficiently protective immune response [34, 66, 63]. This is especially true for oral and aerosol vaccination with killed viruses, which aims to induce protective immunity in the mucosa where most pathogens first enter in the body and constitutes the first line of the immune system's defense [66, 15, 63].

Pharmaceutical companies have chosen not to invest in the development of new adjuvants because they are unlikely to recoup costs. Additionally, the FDA tests vaccine formulations with adjuvants as a single entity and companies are unwilling to risk a vaccine formulation failing because of a previously untested adjuvant. This has led to a lack of new adjuvants to move the field of vaccine development forward. The responsibility to develop and test new adjuvants and vaccination formulations has fallen on academic institutions and independent foundations [63].

1.3 Fowlpox Background

Three viruses were considered as candidates for development of a viral nanoparticle (VNP) vaccine: paramyxovirus, fowlpox, and hemorrhagic enteritis virus. Hemorrhagic enteritis virus and fowlpox were eventually chosen for proof-of-concept experiments because both have significant economic impact in the poultry world, are able to survive a variety of environmental conditions, and are approximately spherical in shape for ease in NP encapsulation.

Fowlpox virus was one of two viruses selected for viral nanoparticle (VNP) fabrication. Fowlpox can cause an egg production drop, slow growth, systemic infection and mortality. Mortality is low for the cutaneous form of pox in which proliferative nodules form, but can be high for the diphtheritic form in which mucosal proliferative lesions form in the nasopharynx and secondary infections or poor environmental conditions can exacerbate the disease. Severe economic losses can result [83, 53, 92, 2]. The current commercially available vaccines are not fully protective against variant fowlpox viruses, leading to some vaccinated flocks experiencing high mortality [83, 53]. Cells of the upper respiratory tract mucosa are highly susceptible to the virus, making a mucosal immunity vaccine an ideal first line of defense. The fowlpox virus itself is typically transmitted through aerosol although it can also be transmitted through lacerated skin, eyes, or via mosquito bites as well. It causes disease in poultry, pet, and wild birds and therefore has worldwide impact. The dimensions of the fowlpox virus are 330 x 280 x 200 nm. This virus is brick-shaped, enveloped, and has random surface tubules. The whole virus is considered the best antigen type for inducing immunity and its targets are the cells of the upper respiratory tract and mouth [6]. The virus is stable to most chemicals, can be heated up to 60^{o}C without being killed, and is stable for months to years in its desiccated state [83, 53]. A representative image of fowlpox is shown in Figure 1.1 below[47].

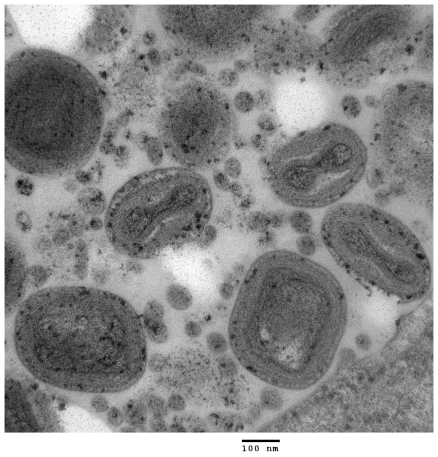

Figure 1.1: Transmission electron micrograph of avian pox virions from a skin lesion in a great tit (Case 4, Sussex, October 2007). Permission to use from Lawson 2012 PLOS ONE.

One of the current commercial fowlpox vaccines is of chick embryo origin and contains live virus capable of producing disease if used incorrectly. The delivery method is via the wing-web stick method, a metal prong dipped in vaccine and inserted into the membranous fold of the bird's wing called the patagium. Each chicken must be individually vaccinated twice for full protective immunity and checked for scabs in patagium post-vaccination. IgA with or without an increase in serum IgG and IgM (hallmark of mucosal immunity) can be increasingly detected 1, 3, 7, and 14 days after inoculation using the wing web stick method. Research on oral vaccination for fowlpox virus has been found to be effective in a German study with an attenuated cell culture vaccine, but other studies found oral vaccination only protected 50% or less of the birds while intramuscular injection, feather follicle inoculation, and intranasal spray delivery methods provided 80-100% protection [83]. The popular method in developed countries is Inovoject (EMBREX, Zoetis; Parsippany-Troy Hills, NJ, USA) technology, which allows mass vaccination of developing embryos within eggs and eliminates the need for individual vaccination but requires high upfront equipment costs. This method uses pigeon fowlpox grown in chick embryo or fibroblasts from cell culture [86, 14, 2]. Based on the available research on fowlpox vaccination, we have determined that fowlpox is a suitable virus candidate for proof-of-concept in creating a vaccine delivery system for killed fowlpox virus using aerosol or water delivery to induce mucosal immunity.

1.4 Hemorrhagic Enteritis Virus Background

The second virus selected was turkey siadenovirus, which causes hemorrhagic enteritis in turkeys and can also lead to immunosuppression, resulting in secondary infections. It can cause depression, melena, duodenal hemorrhage, epithelial necrosis, and splenomegaly. In flocks, morbidity is tends to be 100% and mortality can range from 10-15% with survivors subject to immunosuppression and secondary infection [83, 67, 29, 52]. Due to the insidious nature of this virus, it is difficult to gauge its economic impact. Prior to development of a vaccine, hemorrhagic enteritis caused economic losses exceeding $3 million per year and an additional $40 million per year due to secondary colibacillosis infections in the U.S. Its worldwide economic impact may exceed these numbers, even with vaccination, due to the infection remaining undiagnosed or undetected as a secondary infection to a primary pathogen [83]. HEV is 70-90 nm in diameter, non-enveloped, and icosohedral in shape. While the hexon is the major capsid protein, the whole virus is more immunogenic. The target for the virus is the mucosal-associated lymphoid tissue (MALT), specifically B-cells and macrophages. Immunity after vaccination is nearly immediate and lifelong in duration [67, 52]. The virus is stable to chemical agents, physical stress, and exposure to extreme pH solutions with prolonged survival outside the body. Both virulent and avirulent strains occur naturally [83, 55]. A representative image of the siadenovirus is shown in Figure 1.2 below[22].

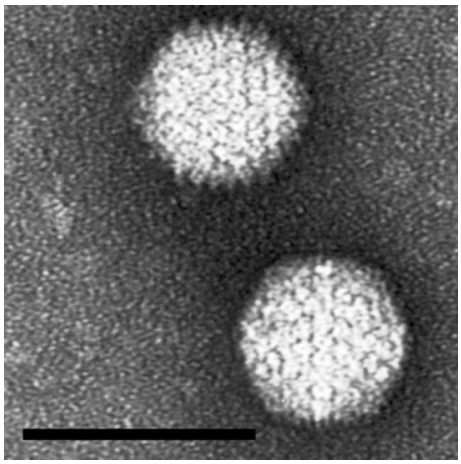

Figure 1.2: Siadenovirus. **Permission to use from Davison 2011 The Springer Index of Viruses.**

An important aspect of the siadenovirus is its protruding fibers made of siaylated surface proteins which is essential for the two-step entry mechanism of this virus into cells. The major function of the fibers is

to interact with the primary adenovirus receptor on the surface of cells and bend to hold the virion at the base of the fiber in proximity to the cell, thus avoiding steric hindrance that would make this interaction impossible otherwise. The virion can then bind to the integrin molecule or other secondary receptor on the surface of the cell, leading to virus internalization. Internalization of the virus causes a cytokine response that leads to apoptosis and subsequent loss of B and bystander cells until immunosuppression eventually results [67, 52]. The delivery system for the siadenovirus must preserve the parts of this two-step mechanism in order for internalization of the virus to occur and subsequently protective immunity to be induced. This interaction is shown in Figure 1.3 below[90].

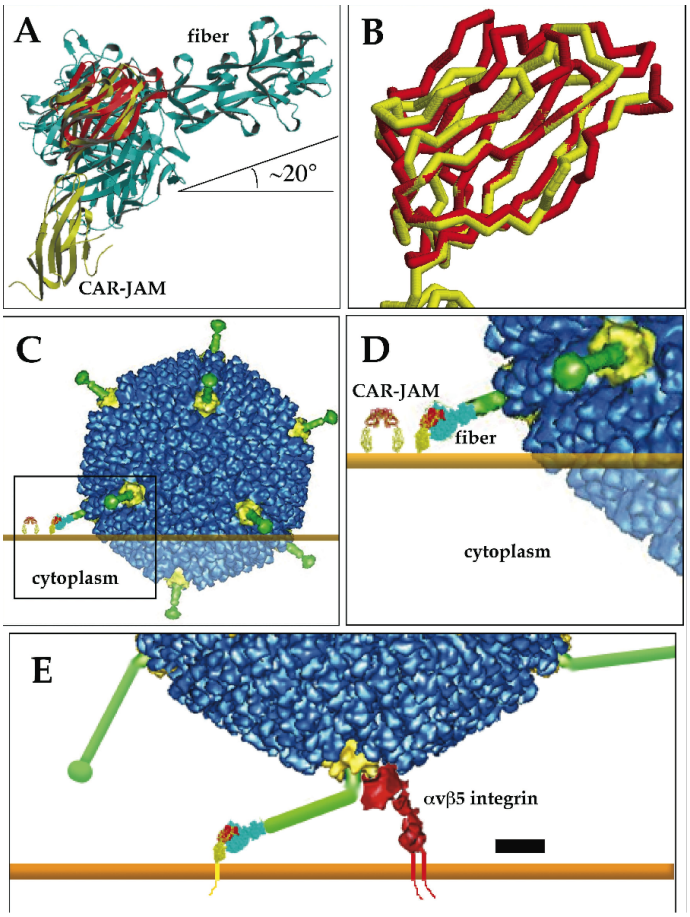

Figure 1.3: Model of Adenovirus (Ad) interactions with cell surface receptors. Panels (A) and (B) show the structure of the fiber, (C) and (D) show the steric hindance that occurs if the fiber is too short, and (E) shows the successful two-step mechanism that occurs when the fiber is long enough and can bend to allow integrin binding. Scale bar, 100 Angstroms. Backbone traces and space filling models in panels B to E were created by using Rasmol 2.7. *citation edited for clarity. Permission to use from Wu 2003 J. Virol.

Siadenovirus has two forms of vaccine currently in widespread use for turkeys. The first is a crude splenic homogenate and the second is adapted/attenuated virus in a cell culture product. Water delivery of the vaccine is the standard method in use in the U.S. and a seroconversion rate of 60% or higher is considered indicative of 100% protection. However, despite high vaccination rates in the U.S., there are still severe outbreaks of HEV called "hot HEV" due to inconsistent protection associated with the cell culture origin vaccine. A second vaccination is recommended for farms where seroconversion has been previously low or if

the cell culture vaccine was used. Most companies have elected to use the crude splenic homogenate due to concerns about the cell culture origin vaccine's efficacy. Due to the nature of the virus, immunosuppression has been noted as a vaccination side effect, leading to secondary infections such as colibacillosis. Many farms choose to use autogenous vaccines, which constitute a regulatory risk and are prone to inconsistency [83, 67].

1.5 Safety Concerns

Both fowlpox and hemorrhagic enteritis virus are species specific viruses and neither has been documented to infect humans. They are classified as BSL1 viruses and in these studies were worked on under BSL2 conditions. Additional safety measures include using a 0.02% paraformaldehyde fixative to kill the virus prior to encapsulation in nanoparticles, working in a biosafety cabinet for fabrication, and transporting viral NPs in sealed and parafilmed containers with the outside wiped down with 10% bleach and 70% ethanol [53, 83, 24, 18, 8].

1.6 Previous Literature Approaches

1.6.1 Fowlpox Vaccine Research

The current research surrounding fowlpox vaccination relies on using the fowlpox vector or virus for injectable vaccines to protect against fowlpox or other viruses in the case of recombinant vaccines and does not address the need for less labor intensive, mass vaccination strategies for food animals in veterinary medicine [33, 87, 17]. Published research on formulating a new fowlpox vaccine is limited to using whole virus with no delivery vehicle and has found that fowl pox dust, spray and intraperitoneal delivery produced good immunity while intra-ocular inoculation and cloaca or throat swabbing did not [31]. By contrast Nagy, *et al.* found that administering a 10^4 mean cell-culture infectious dose ($CCID_{50}$) per mL using aerosol or water delivery of a plaque-purified derivative of a commercial fowlpox vaccine yielded inconsistent serological results and did not provide protective immunity until high viral loads (10^6 $CCID_{50}$ per mL) were used while cutaneous administration with the lower dose (10^4 $CCID_{50}$ per mL) did yield protective immunity [60]. We hypothesize that using gelatin and chitosan as polymeric adjuvants will enable killed virus to stimulate protective immunity with an oral delivery vaccine. Achieving this would allow this vaccination to be converted

from the more laborious injectable method to aerosol or oral delivery.

1.6.2 Hemorrhagic Enteritis Vaccine Research

The siadenovirus genus was discovered relatively recently in 2002 and before that was known as group II avian adenovirus. Most published research has focused on finding identifying and distinguishing characteristics of this virus and its strains [52, 45]. Hemorrhagic enteritis virus (HEV) isolates from vaccinated turkey flocks with increasing secondary bacterial infections are being gathered to determine whether the current HEV vaccines are losing efficacy, which may be due to new viral strains emerging [3]. During development of a stationary cell culture to propagate HEV efficiently with peripheral blood leukocytes infected with crude spleen extract, purified spleen extract, or cell-culture-produced HEV, the mean tissue culture infectious dose was found to be within 5-20 $TCID_{50}$ per mL. An HEV hexon (major outer capsid protein) protein subunit vaccine was investigated to determine whether it could produce hexon-specific antibodies in sera, protect against clinical disease, and prevent viral replication after a virulent HEV challenge in turkeys. Provided the hexon was not denatured, the injectable vaccine was able to successfully fulfill the three outlined criteria and protect against hemorrhagic enteritis. However, production of the purified hexon was found to be cost prohibitive for mass vaccine production [37]. The remainder of the literature is limited to adenovirus (with or without recognizing siadenovirus within that group) and uses the virus as a vector to carry other biologics such as genetic material [56]. Water-based delivery siadenovirus vaccines are already commercially available, making this virus an attractive candidate for testing a new water-based delivery system as proof-of-concept prior to converting other vaccines [83].

1.7 Proposed Approach

1.7.1 Oral Vaccination and Induction of Mucosal Immunity

1.7.2 Oral Adjuvant Candidates

After review of the needs in the poultry industry and the literature available on developing new fowlpox and hemorrhagic enteritis vaccines, new adjuvants constitute the key design element for enabling creation of a new non-injectable vaccine delivery system capable of inducing protective immunity. In designing this proposal,

the literature was reviewed to determine the best type of adjuvant for creating a new vaccine delivery system applicable to fowlpox and hemorrhagic enteritis formulations. The most commonly used adjuvant, aluminum salts, is not effective on mucosal surface and can cause side effects like inflammation or granuloma-formation, making it contraindicated for vaccines delivered to the mucosa [15, 79]. Oil emulsions have previously been used successfully, cause less tissue reactivity and granuloma formation, are considered suitable for a mucosal delivery vaccine, and have been recommended for poultry vaccination formulation where long-term immunity is needed [15, 13]. However, using a spray/aerosol to deliver an oil emulsion vaccine would negatively affect the thermoregulatory abilities of the chick/poult and could potentially cause aspiration pneumonia, which restricts administration to eyedrop delivery and requires an overly labor-intensive delivery method. Immunostimulatory complexes (ISCOMS) are immunostimulatory fractions from Q saponaria that are incorporated in lipid particles made of cholesterol, phospholipids, and cell membrane antigens. ISCOMS produce particles in the 30-40 nm range capable of inducing 10-fold greater antibody responses than other adjuvant vaccines. ISCOMS have successfully been used with Newcastle virus in chickens and avian influenza virus in turkeys, but their cost of production is high, injection site reactions have occurred, and toxicity can occur with some saponin preparations [15, 79, 85]. Liposomes have been used for the same viruses and species as ISCOMS in poultry medicine, but their use is limited due to lack of stability and the use of organic solvents, which can damage the antigens during vaccine production. Other adjuvants have limited data and would not be suitable for oral delivery in poultry until further research has been done on their formulation and safety in food animal species [15].

Polymeric Adjuvants

Natural polymers were considered as candidates for vaccine adjuvants as they are biodegradable and many do not elicit strong adverse immune reactions when introduced to the body [15, 13, 71, 9, 21]

The use of alginate nanoparticles would require challenge models to determine efficacy and, additionally, have previously had inconsistent uptake in vaccine formulations. [65, 23, 72]

Aliphatic polyester (PLGA, PLA, PGA) particles have been used in veterinary vaccine formulations with promising results for mucosal delivery [15, 26]. The materials are already FDA-approved in humans as sutures and as biocompatible and biodegradable drug delivery systems. They have well characterized hydrolysis rates, last up to one year with sustained antigen release, and are readily phagocytized by macrophages and antigen

presenting cells. Additionally, they can be lyophilized to make vaccines usable in areas where refrigeration is not possible, and the particles have the potential to induce long lasting immunity using polymers of differing molecular weights or particles of different sizes to avoid the need for booster vaccinations [15, 79, 26, 35, 89]. Previous research with Salmonella enteritis vaccine used a 50:50 PLG and PLA microparticle preparation and was successful in stimulating the immune system for 9 months [15, 89]. PLGA particles (of nano or micron-size) may be included to ensure a sufficient immunostimulatory dose and sustained release of the virus to the immune system if indicated. We had included them in our proposal as a second option for preparation of viral nanoparticles but in the course of this work chitosan emerged as a better option based on the literature and experimentation [69].

Chitosan is a cationic polysaccharide derived from chitin, a natural polysaccharide extracted from shellfish. Due to the cationic charge from protonated amino groups, chitosan has adhesive properties for anionic surfaces, including mucus and proteins. Chitosan has been used to enhance oral and nasal delivery of antibiotics, antihypertensive agents, DNA, peptide drugs, vaccines and proteins [69, 41, 19, 51, 6, 11, 42, 44, 10, 50, 68] . Although the mechanism is not fully elucidated, it is believed to be due to increased uptake from transient opening of intercellular tight junctions, which both improves uptake of macromolecules and slows mucociliary clearance. Ultimately, this increases the bioavailability of the delivered antigen[69, 93, 19, 6, 11, 10, 50]. Chitosan has been purported to stimulate the immune system through attracting and activating macrophages and polymorphonuclear cells, induction of cytokines and antibodies, and enhancing delayed-type hypersensitivity reactions via the Th1 pathway and cytotoxic T-lymphocyte responses leading to both enhanced mucosal and systemic immune responses [51, 6, 68, 69]. Animal studies using chitosan as a mucosal adjuvant have found enhanced vaccine efficacy and protection [11, 82, 39, 10]. A study in which chickens were given a single dose of live Newcastle disease virus adjuvanted with 0.5% chitosan via oculo-nasal delivery found the use of chitosan significantly increased cell-mediated immunity at the splenic level, an increased peripheral cellular immune response developed earlier, and the Th1 pathway of immunity was enhanced [69]. Based on these findings in the literature, chitosan was chosen as one of the polymer mucosal adjuvants for this body of work.

Gelatin was selected as the other mucosal adjuvant because as a natural polymer derived from collagen, it is generally recognized as safe (GRAS-certified) by the FDA and is inexpensive as a material [**2008**, 46, 40, 49, 27, 28]. Gelatin has a long history of safe use in pharmaceuticals, cosmetics, and food products. It contains functional groups such carboxylic acids, amines, and hydroxyl groups that can be easily chemically modified

to aid in targeted delivery, and is already in use in clinical settings [31, 40, 27, 28, 32]. As an adjuvant, gelatin enhances uptake of nanoparticles and the immunostimulatory ability of encapsulated antigen, specifically via upregulation of MHC II and CD86 molecules on dendritic cell surfaces leading to more T cell activation and priming [94, 81]. Gelatin is also reported to have an opsonic ability for macrophage phagocytosis, meaning the gelatin facilitates delivery of a large amount of antigen to macrophages which then are stimulated and cause increased secretion of lymphokines and nonspecific cytotoxicity [61].

When used in the double desolvation technique with chemical crosslinkers like glutaraldehyde, glyceraldehyde, and genipin to form NPs, it is believed to form a net-like structure that can encapsulate larger materials and allows smaller materials to adsorb to the surface of the NP [40, 88, 78]. An illustrative schematic is shown in Figure 1.4 below[49].

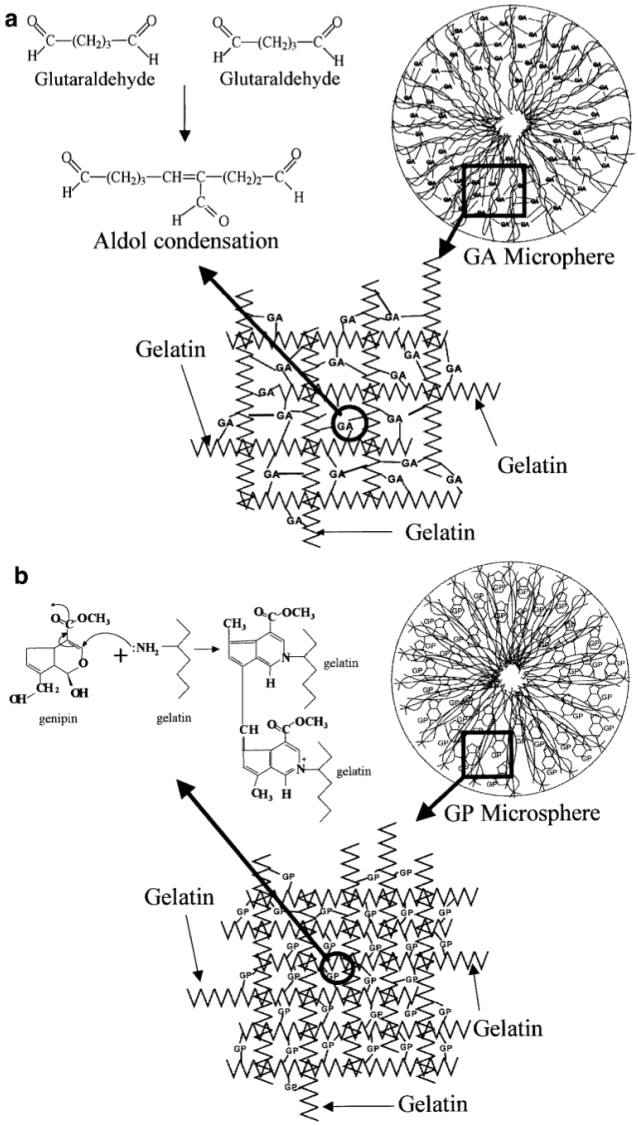

Figure 1.4: Schematic illustrations of the presumable crosslinking structures of (a) the glutaraldehyde-crosslinked gelatin microspheres and (b) the genipin-crosslinked gelatin microspheres. GA, glutaraldehyde; GP, genipin. Permission to use from Sung 2003 J Biomed Mater Res A.

1.7.3 Rationale

Based on the literature, we have elected to choose whole virus as the antigen for our vaccine delivery system, gelatin as our polymeric adjuvant with chitosan as an additional polymeric adjuvant, an oral water-

based delivery method, and to target poultry (chickens and turkeys) as our population of interest for the proof-of-concept experiments. We chose whole virus because our processing methods will expose the virus to paraformaldehyde as a chemical fixative, which must kill the virus but also preserve the whole virus for immune cell and antigen presenting cell (APC) recognition and uptake, culminating in antibody development and protective immunity during challenge. Additionally, the siadenovirus has a detailed mechanism for uptake that requires an intact outer fiber capable of bending for entry in the cell that would likely be disrupted with a subunit antigen [83]. Nano-sized particles will be formulated to closely match each virus' size and target macrophages, histiocytic cells, dendritic cells, and APCs present in the mucosa to increase nanoparticle uptake as has been documented by others [17, 40, 71, 30, 61, 74, 57, 77, 20, 48, 43]. This ability of NPs allows them to deliver a high concentration of a pharmaceutical agent to the desired target and is called engineered specificity [12]. Using two different polymers allows the option of mixing polymeric nanoparticle types to achieve the best nanoparticle properties. Gelatin is GRAS-certified and chitosan has been used in humans as a dietary fiber, health and food applications, and for antigen delivery [15, 13, 71, 9, 21, 11, 19, 93, 68]. Both are biocompatible, biodegradable, and elicit minimal side effects in the mucosa [15, 13, 71, 9, 21, 11, 82, 19, 41, 93]. Gelatin and chitosan are inexpensive and the simple double desolvation technique is easily scalable for larger production [40, 71]. The delivery method will mimic the same entry method that the wild-type virus uses to infect in hopes of stimulating better protective immunity. In using killed virus formulations, we hope to avoid undesirable side effects seen with the current vaccines on the market in which the virus can actively replicate. We will start with the turkey hemorrhagic enteritis vaccine for clinical and challenge studies because this virus already has a water-based vaccine on the market and therefore likely has the highest chance for success for proof-of-concept. After proof-of-concept is established, we hope it will lay the groundwork to improve the fowlpox vaccine by changing the vaccination to aerosol or water delivery, thereby showing that the vaccine delivery system can be applicable to multiple viruses.

1.7.4 Double Desolvation Fabrication Mechanism and Underlying Concepts

The double desolvation technique was chosen to produce the nanoparticles because of its inexpensiveness, ability to fabricate large quantities of nanoparticles in a short period of time, batch-to-batch reproducibility, and scalability [40, 71]. The technique is relatively easy to learn and can be used in laboratories lacking expensive equipment. These characteristics make it an attractive method for a veterinary product [12]. The technique is amenable to additions such as dyes, different encapsulation materials, and different crosslinkers

as needed to customize the product to the biomedical application. The term "desolvation" refers to removing solvating water molecules using a non-solvent from the hydration shell of a macromolecule, which are the polymers in this case. Gelatin has the characteristic collagen triple helical conformation. This conformation is attributed to the Gly-X-Y repeat conserved throughout the protein. The other major amino acids include hydroxyproline, proline and alanine. This unique makeup of gelatin allows for its unusual hydrogen bonding which in turn is responsible for its high water retention capacity [1]. Gelatin NP degradation can be through either bulk degradation or surface erosion with the major mechanism of release attributed to protease-degradation [40]. The mechanism of the desolvation process is harder to identify because it appears to be dependent on pH as seen in Figure 1.5 [1].

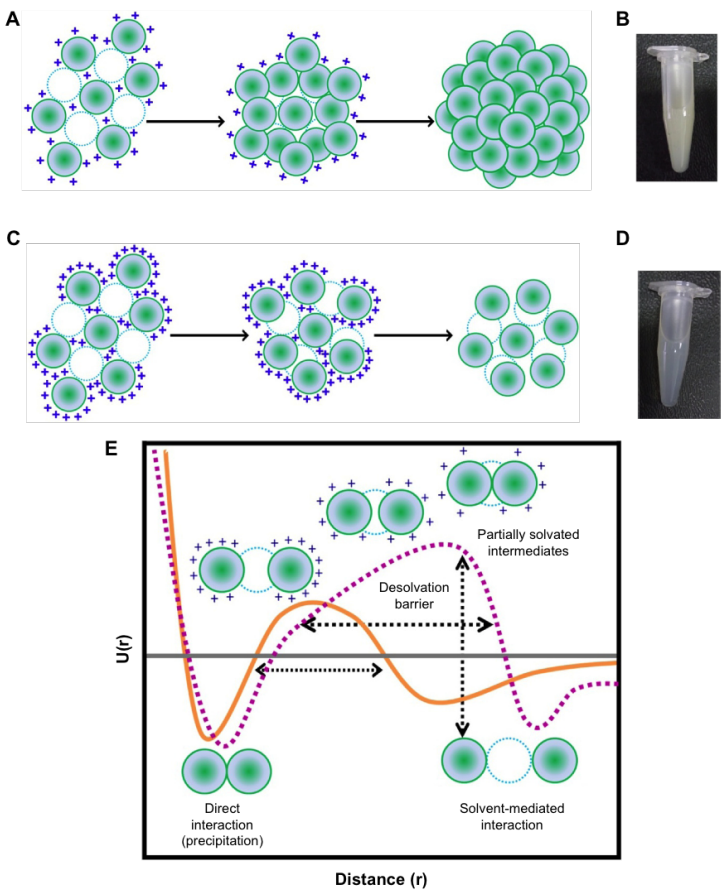

Figure 1.5: Mechanism of GNP synthesis at (A) pH 4 and (C) pH 3.25. Micrographs of GNPs synthesized at (B) pH 4 with HMD and (D) pH 3.25 with LMD (E) Schematic representation of potential energy function (U(r)) in the desolvation model. In this model, a native interaction between two gelatin residues (green spheres) can be either direct or mediated by a water molecule (blue dashed circle). Orange curve represents the potential energy function for gelatin protein during desolvation. Dashed purple curve represents the potential energy function for gelatin under conditions of nanoparticle synthesis. The "+" represents the positive surface charge on the molecule ([E] Adapted from Cheung MS, Garcia AE, Onuchic JN. Protein folding mediated by solvation: Water expulsion and formation of the hydrophobic core occur after the structural collapse. Proc Natl Acad Sci USA. 2002; 99[2]: 685-690. Copyright [2002[National Academy of Sciences, USA.) Abbreviations: GNPs, gelatin nanoparticles; HMD, high matrix density; LMD, low matrix density. Permission to use from Rao 2017 Int J Nanomedicine.

The isoelectric point (pI) of Type A gelatin is pH 7-9 while the pI for Type B is pH 4.7-5.4. The pI for proteins refers to the pH range where the protein's net charge is zero. If the pH is less than the protein's pI, then protein will be positively charged. If pH is greater than the pI, the protein will be negatively charged [5]. Having sufficient positive or negative surface charge in solution is essential for intermolecular repulsion to occur and prevent NP aggregation. For NPs in a vaccine formulation, positively charged NPs are preferred because they are more likely to be picked up by the mononuclear phagocyte system and generate a higher immune response than neutral or negatively charged NPs. Electrostatic interactions were used to coat the gelatin nanoparticles with chitosan to ensure a large positive charge at acidic pH. Additionally, NPs with diameter greater than 10 nm will avoid rapid clearance via the kidney or extravasation [12]. NP formation in acidic environments is preferred to produce NPs of reproducible diameter and small size distribution (PDI). The desolvation process is believed to consist of two phases. In the first phase, the NP size increases with increasing acetone (desolvating agent) concentration. In the second phase, the number of particles increases with increasing acetone concentration. An increase in PDI is also seen in this second phase and is attributed to addition of free gelatin to preformed NPs, further removal of water from the preformed NPs, and interparticle aggregation due to low surface charges. When the controlled desolvation process occurs at pH 4, it is believed that the first phase creates a dense gelatin core for additional gelatin to form around. This process is seen in Figure 1.5 (B). The NPs formed are considered to have high matrix density (HMD). When controlled desolvation occurs at pH 3.25, the mechanism for NP formation appears to be that large initial NPs form at low acetone concentrations and then as the acetone concentration increases, these NPs condense down to a smaller diameter. Overall, NPs formed at pH 3.25 appear to have low matrix density (LMD) compared to NPs produced via the previous mechanism which have a high matrix density (HMD). In this way, the determining factors for matrix density are pH and acetone concentration [88, 1]. The proposed potential energy model agrees with the desolvation barrier model that suggests the protein folding seen in the desolvation process takes place through a partially hydrated and less stable state. The two minima in Figure 1.5 (E) are thought to be a stable hydrated state and a precipitated state in the gelatin NP fabrication process. NPs in between these two favored states are energetically unstable and tend to aggregate or dissolve without chemical crosslinking to preserve them [1].

1.7.5 Basis for Nanoparticle Characterization

Based on the mechanism previously outlined, the NP solutions produced can consist of both HMD NPs, NPs that fall between HMD and LMD, and LMD NPs if the pH is not continually controlled and changes slightly from 3.25 to 4 due to addition of the desolvation agent. When the majority of NPs are HMD, the solution will be turbid while LMD NP majority solutions are clearer. These color changes agree with our own observations of the double desolvation process. However, gelatin NP solutions are considered colloidal due to having an approximate side range within 1-1000 nm. The basis for the color change comes from the Faraday Tyndall Effect and the scattering of light allows for dynamic light scattering analysis to determine the basic properties of each colloidal solution [52]. With the assumption that the NPs are roughly spherical, Stokes-Einstein equation applies, allowing the NP diameter and size distribution (PDI) to be measured using dynamic light scattering in addition to ZP (surface charge). NP solutions must meet the quality limits set for these three parameters before they can be used in subsequent experiments for vaccine formulation.

$$D = \frac{kT}{\pi \nu D_{\mathrm{H}}}$$

Figure 1.6: Stokes-Einstein Equation where D is the diffusion speed, k is Boltzmann's constant, T is the absolute temperature, ν is the viscosity, and $\mathbf{D_H}$ is the hydrodynamic radius. This equation is based on the assumption of Brownian motion that states that small particles dispersed in solution are constantly bombarded with solvent molecules. These solvent molecules are in constant motion due to thermal energy which results in collisions with the small particles. The speed of the Brownian motion can be directly measured according to the scattered light pattern produced by the moving particles.

1.8 Conclusion and Aims

To our knowledge, a polymeric approach with encapsulated whole virus had not been used for fabrication of either fowlpox or hemorrhagic enteritis vaccines. This approach was cost-effective compared to using other more expensive adjuvants or antigens, applied well documented methods to new vaccine formulations, used minimal lab equipment, and had a novel adjuvant to stimulate protective mucosal immunity. Both of the proposed vaccine formulations constitute proof-of-concept and open the door for the NP delivery system to

be applied to other viruses, polyvalent vaccines, drugs, and other biological materials.

We elected to create both a FPV nanovaccine for oral/aerosol delivery and a HEV nanovaccine for oral delivery. Both virus formulations were tested for basic NP properties, cytotoxic effects on appropriate cell lines, and viral release/uptake. The HEV nanovaccine was selected for clinical and challenge animal studies due to the virus being amenable to water delivery as evidenced by the current commercial vaccines. The HEV nanovaccine served as proof-of-concept prior to attempting to convert fowlpox and other injectable vaccines to oral or aerosol delivery. The following aims guided this research:

- **Aim 1: Could reproducible stable nanoparticles encapsulating inert materials of similar size and shape to fowlpox virus and hemorrhagic enteritis virus be fabricated?**
  The basic properties of each NP type were investigated. The average diameter, width of the size distribution (polydispersity index, PDI), and zeta potential (surface charge) of each NP type were measured using dynamic light scattering. The ideal parameters for each NP formulation were to have initial average diameter close to the encapsulation material in order to facilitate cellular uptake by the populations of interest, a PDI less than 0.1 for highly controlled encapsulation or at least less than 0.2 for less controlled encapsulations, and to have an initial ZP close to -30 mV or + 30mV at pH 3-4 to avoid NP aggregation in solution. Additional properties that were investigated included NP morphology and types of encapsulation using transmission electron microscopy (TEM), stability under freeze/thaw conditions, and stability over the physiological pH range that may be encountered in the body.

- **Aim 2: Could the NP delivery system be modified to minimize cytotoxicity in chicken fibroblasts and turkey lymphoblastoid cells *in vitro* studies?**
  NP cellular uptake and cytotoxicity were tested using chicken fibroblasts and turkey lymphoblastoid cells for the fowlpox VNPs and turkey siadenovirus VNPs, respectively. Timed confocal microscopy with fluorescent staining and transmission electron microscopy (TEM) were used to ascertain whether the NPs were taken up by both cell lines. Lactate dehydrogenase (LDH) cytotoxicity and (3-(4,5-dimethylthiazol-2-yl)-5-(3-carboxymethoxylphenyl)-2-(4-sulfophenyl)-2H-tetrazolium) (MTS) Cell Proliferation assays were used to quantify cytotoxicity and cell viability. Centrifugation, washing, filtration, and lyophilization were employed to concentrate, purify, and sterilize the NP formulations.

- **Aim 3: Could reproducible stable nanoparticles encapsulating fowlpox virus and hemor-**

rhagic enteritis virus be fabricated, could they be taken up by the appropriate immortalized avian cell lines, and did their viral release have a cytopathic effect?

The basic properties of the viral nanoparticles (VNPs) were investigated using similar methods to Aim 1. TEM imaging and timed confocal microscopy studies with fluorescent staining were performed to confirm cellular uptake of the VNPs. Quantitative PCR for viral DNA were used to determine whether the siadenovirus could still replicate after VNP degradation and viral release. The virus' genome copy number did not increase, indicating the virus was successfully killed during VNP processing. Without the ability to replicate, the virus was unable to deplete splenic immune cells and therefore unlikely to cause immunosuppression.

- **Aim 4: What were the immunological effects of the turkey hemorrhagic enteritis nanovaccine on the immune cell populations of interest?**

  Clinical and challenge studies were performed using the hemorrhagic enteritis nanovaccine. The clinical study compared the immunity induced from the killed HEV nanovaccine to that of the killed HEV with loose gelatin and chitosan polymers (no nanoparticle), and that of a live HEV vaccine. Antigen processing of the killed HEV with loose polymers formulation was efficient and germinal center counts correlated with significant detectable antibody development but no detectable significant antibody development was found for the HEV nanovaccine. Serum antibody titers were measured post-vaccination using a standard enzyme-linked immunosorbent assay (ELISA) methodology to determine seroconversion. Immunity should be highly dependent on antigen-presenting cells (APCs) like macrophages, histocytes, and dendritic cells in mucosa-associated lymphoid tissue (MALT). For the challenge study, body-to-spleen ratios were calculated to determine whether each vaccination type was able to protect birds from infection after challenge with live virus. The spleen is the site of replication for hemorrhagic enteritis virus and the degree of splenomegaly has been found to be proportional to viral dose as well as the most reliable measure of infection. The body-to-spleen weight ratio is the most consistent parameter for measuring viral activity. While the exact mechanism is still being elucidated, there is evidence infection of macrophages and B cells in the spleen may lead to migration of additional macrophages and CD4+ T cells in the splenic white pulp, eventually resulting in white pulp hyperplasia[24, 64, 25]. Real-time qPCR was performed on splenic samples to measure viral clearance and confirm body-to-spleen ratio data. Histopathology, number of geminal centers per high power field, and gross examination of the turkey spleens were performed to determine if other tissues had vaccine-induced side effects

and to confirm whether protective immunity had been induced. For the HEV with polymers group, virus genome copy number did not increase (from Aim 3) while antibody production was seen and the body-to-spleen ratio was significantly larger than that of unvaccinated birds. This was indicative HEV's two-step uptake mechanism was intact and the outer capsid and fiber were preserved during fixation and processing. All together, this constituted proof gelatin and chitosan were able to induce protective immunity as polymeric adjuvants with a killed virus water delivery vaccine. A significantly higher body-to-spleen ratio is the gold standard to show vaccine protection with HEV and indicates the virus was unable to replicate but still induced protective immunity. This result was confirmed using the actual amount of virus still present in the spleen measured with qPCR to demonstrate faster viral clearance during the challenge study for vaccinated birds.

- **Deliverables**

  The deliverables from this project included fowlpox nanovaccine; hemorrhagic enteritis nanovaccine stability data on both types of VNPs; data on viral release and interaction with the cell populations of interest; and immunological, histological, and gross pathological assessments of two HEV vaccine formulations to demosntrate safety and efficacy. As the HEV loose polymer formulation showed seroconversion and protective immunity equal to the live commercial HEV vaccine, the oral fowlpox nanovaccine should be tested in vivo for future work.

Chapter 2

Simple and Customizable Gelatin Nanoparticle Encapsulation System for Biomedical Applications

This paper has been submitted to *Journal of Nanomaterials and Molecular Nanotechnology* and is under review. The work shown encompasses Aim 1.

2.1 Abstract

The double desolvation technique has been used to encapsulate small, hydrophilic drugs with protein affinity in gelatin nanoparticles for many years. Expanding the types of materials that can be encapsulated would allow the double desolvation method to be used for a wider range of biomedical applications, including biological delivery. Here, we use the double desolvation technique to encapsulate two different sizes of polystyrene beads as a first step toward encapsulating biologics like viruses and nucleic acids of similar size, shape, zeta potential, and functional groups in a new delivery system. Drug delivery systems that are easy to produce and customizable to different biomedical applications are in demand. With these parameters in mind, we created a simple gelatin nanoparticle encapsulation system with the potential for chemical modification for targeting purposes and encapsulation of different materials. Matching the encapsulation material to the size and shape of the empty nanoparticles resulted in encapsulated nanoparticles of an ideal narrow size distribution with stable storage parameters at room temperature over a 1-month period in distilled water. Additionally, the encapsulation system was shown to be most stable at pH 3-4 compared

to other physiological pH ranges. Transmission electron microscopy verified the size ranges found using dynamic light scattering and revealed the inert material was encapsulated, partially encapsulated, and non-encapsulated nanoparticles in each formulation. This matched encapsulation material fabrication method may decrease the need for additional filtration after biologics are added and the encapsulation range would be ideal for sustained biologic release over time.

2.2 Introduction

Major advances in modern day drug delivery systems have been controlled release formulations and specific targeting to the tissues of interest. Formulations with these characteristics have increased therapeutic effectiveness, reduced administration frequency, and reduced side effects related to repeat dosing [9, 21, 71, 30, 40, 74, 88, 59, 57, 73, 77]. Delivery systems must be simple to produce, customizable, and inexpensive to be viable alternatives to the conventional delivery methods already in use in healthcare [40, 74, 75, 7]. To date, the majority of biologics encapsulated in gelatin for therapeutic purposes have been small drugs of <5 nm diameter [91, 46, 12]. Our goal in this project was to encapsulate larger materials in a gelatin nanoparticle (NP) system as a first step toward a new delivery system of larger biologic materials. To ensure the system was simple to produce and easily adaptable to customer needs, inexpensive materials were used and the lab equipment required was kept simple, so the system could be produced in a wide range of laboratories at minimal cost [71, 40, 88]. NPs can be used to deliver a variety of encapsulated materials, including drugs, polyphenols, RNA, genes, proteins, and viruses allowing for NP delivery systems to be used across the medical field in different biomedical applications [9, 71, 30, 78, 16]. Using nanoscale particles can lead to enhanced uptake by cell populations of interest, such as macrophages, M cells, and tumor cells [71, 30, 40, 74, 88, 57, 77, 20, 48, 43]. Gelatin was chosen to form the NP polymer shell because it is a natural polymer that is widely biodegradable into benign components, generally recognized as safe (GRAS)-certified, already in use in the medical field for various applications, inexpensive, and has many functional groups that can be modified for targeted drug delivery [9, 40, 88, 57, 20, 32, 62]. NPs can be used to prolong the delivery of encapsulated materials with otherwise low bioavailability or with short half-lives [40, 59, 16]. NPs may also be targeted to tissues that historically have been difficult to reach and can achieve sufficient therapeutic drug doses using systemic drug delivery. We chose to use polystyrene beads of two different sizes, 100 nm and 200 nm, as inert encapsulated materials for ease of initial characterisation of the system. In later work,

these stand-in materials will be replaced by biologics of similar size, shape, zeta potential, and containing similar functional groups as the system is modified for different biomedical applications. Controlling the size of NPs allows for targeting the delivery system to particular tissues or cells and should further targeting ability be required, the reactive groups on the gelatin may be modified [9, 40, 88, 57]. Overall, this system has the potential to expand NP delivery to biologics larger than conventional drugs. Our hypothesis is that matching the encapsulated material diameter to the empty nanoparticle diameter will produce the best combination of encapsulated nanoparticle parameters: a diameter close to the encapsulated material diameter, a narrow and monodisperse size distribution (polydispersity index, PDI), and sufficient particle charge (zeta potential, ZP) to avoid particle aggregation. The ideal specifications for NPs in this study were to have encapsulated NPs of similar initial average diameter to the encapsulation material (100 nm and 200 nm) in order to facilitate cellular uptake, to have the initial average size distribution less than 0.1 for highly controlled encapsulations or at most 0.2 for less controlled encapsulations, and to have an initial average ZP close to 30 mV at a storage pH of 3-4 to avoid NP aggregation [40, 88, 59, 78, 20]. Additionally, the NPs should no statistically significant changes in diameter or size distribution for at least one month at room temperature in distilled water as an indicator of product storage stability.

2.3 Materials and Methods

Two types of gelatin, Type A 300 Bloom (Sigma-Aldrich; St. Louis, MO) and Type B 275 Bloom (Vyse Gelatin Company; Schiller Park, IL) were used in the two step desolvation NP fabrication process. These polymers have been characterised in previous literature [24]. Polystyrene PolyBead beads (100 nm average diameter) and Fluoresbrite beads (200 nm average diameter) were used as encapsulation materials (Poly-Sciences, Inc.; Warrington, PA) as they have anionic charges from their sulfate ester groups similar to those found in biologics like proteins and nucleic acids. The two gelatin types were selected because their NP sizes could be consistently and repeatedly produced [24]. Glutaraldehyde (25%, Sigma-Aldrich; St. Louis, MO) was used for all NP crosslinking. All other materials were analytical grade and used as received.

2.3.1 Nanoparticle Preparation

A two-step desolvation method was used to make the nanoparticles in which an organic desolvating agent caused aggregation of the gelatin molecular chains around the encapsulation material of interest with chemical crosslinking for stability [9, 73, 80]. Briefly, gelatin was dissolved in distilled water with stirring at 600 rpm and heated until solution was clear and light yellow (42 °C for Vyse 275 Bloom and 39.5 °C for Sigma 300 Bloom). The solution was removed from heat and acetone (25 mL) was added to allow separation of high molecular weight (HMW) and low molecular weight (LMW) gelatin chains to decrease the variability in gelatin used to create the NP suspension. After 24 hr at room temperature, the top LMW liquid gelatin layer was decanted and the bottom HMW solid gelatin layer was redissolved in distilled water with the same stirring and heating parameters as above. The pH was adjusted to 2.5 using 1M HCl and then 9.1 x 10^{12} polystyrene beads (100 nm or 200 nm) were added. The stirring rate was increased to 1000 rpm to ensure homogeneous dispersion of the insoluble beads. Acetone (70 mL) was added dropwise using a syringe pump (3 mL/min) while the solution temperature was maintained (37-39.5 °C for Sigma 300 Bloom and 40-42 °C for Vyse 275 Bloom). An iridescent blue colour change from the Tyndall effect was observed, indicating nanoparticle formation as the gelatin encapsulated the polystyrene beads. Excess acetone (5 mL) was added and then the beaker was moved to a stir plate without heat for 5 min (600 rpm). Glutaraldehyde (25 wt % in water, 250 µL) was added in a single injection and the colloidal suspension was left to crosslink over 24 hr. After crosslinking, the sample was concentrated by rotary evaporation using an RV 10 digital V (IKA; Wilmington, NC) to remove acetone until 25-30 mL of suspension at pH 3-4 remained over 40-60 min. An aliquot of the sample suspension 100 µL) was diluted into deionized water (900 µL) in a plastic cuvette and three measurements were taken to estimate the average diameter, size distribution and ZP of each sample using cumulants analysis with a Zetasizer- Nano-ZS (Malvern instruments; Southborough, UK). The remainder of the sample suspension was stored at room temperature.

2.3.2 Nanoparticle Stability Characterization

NPs fabricated from the initial diameter studies, were used to determine stability under room temperature storage, freeze/thaw cycle conditions, and under varying pH conditions. For the storage study, samples from each batch of NP formulation were stored at room temperature in distilled water and aliquots measured weekly for average diameter and PDI over the course of a month. For the freeze/thaw study, each suspension

was measured as above and frozen for 48 hr, and then thawed completely prior to measuring the diameter and PDI again to determine the effect of a single freeze/thaw cycle. A short 5-day study on the effect of a physiological pH range was also investigated. One molar hydrochloric acid and 0.5 M NaOH were used to adjust the NP suspensions from a baseline pH of 3-4 to the desired pH ranges of 1-2, 5-6, and 8-9. The average diameter, PDI, and ZP were measured daily for each of the pH ranges.

2.3.3 Nanoparticle Imaging

Transmission electron microscopy (TEM) were used to determine the types of encapsulation present in the NP suspensions. A blue FD&C dye was used to stain the gelatin during fabrication just prior to the addition of drop-wise acetone to aid sample visualisation. The NPs were dehydrated in 100 % ethanol for 4 hr, filtered onto a nanocellulose membrane, and dried with a LADD critical point dryer overnight. The NPs were stained with lead citrate prior to imaging with a JEOL JEM-1400 Transmission Electron Microscope (JEOL Ltd.; Japan).

2.3.4 Statistical Analysis

One-way ANOVA analysis was used to determine whether significant differences existed between sample groups. When significance was present, Tukey's HSD Test was used to reveal which samples were significantly different. JMP Pro Software (v. 12.0.1, SAS Institute Inc., Cary, NC) was used for all statistical analysis. Data are reported as averages ± standard error with three replicates.

2.4 Results and Discussion

2.4.1 Initial Nanoparticle Characterisation

For initial NP fabrication, two polystyrene bead sizes and two types of gelatin were used for encapsulation. The basic properties of the 100 nm and 200 nm polystyrene beads designated as PS100 and PS200, respectively, in deionized water at a pH of 5 are shown below in Table 1.

Table 2.1: Properties of 100 nm (PS100) and 200 nm (PS200) polystyrene beads. One sample was measured three times for each polystyrene bead type and values are reported as the average ± standard deviation. (n = 3 measurements).

Nanoparticle Type	Average Diameter (nm)	Average PDI	Average ZP (mV)
PS100	108.07±1.70	0.022±0.021	−57.50±0.72
PS200	215.63±0.93	0.019±0.005	−56.80±0.82

If the encapsulated material diameter closely matched the empty NP diameter, then the encapsulated NP is considered matched for the purposes of this work. Sigma Type A 300 Bloom gelatin is designated as G300 while Vyse Type B 275 Bloom gelatin is designated as G275. G300 and G275 designated empty NP fabrications, G300PS200 and G275PS100 were matched encapsulated NPs, and G300PS100 and G275PS200 were non-matched encapsulated NPs. Three batches of each NP type were averaged to calculate the as fabricated NP parameters in Table 2.

Table 2.2: As fabricated properties of NP types measured using DLS. Sigma Type A 300 Bloom (G300), and Vyse Type B 275 Bloom (G275) gelatin were used to encapsulate 100 nm (PS100) and 200 nm (PS200) polystyrene beads. Three samples of each fabrication type were measured three times each and the values are reported as the average standard deviation (n = 3). The asterisk, section sign, diamond, cross, and double dagger (∗, §,♦,†,‡) indicate significant differences between fabrications (p<0.05).

Nanoparticle Type	Average Diameter (nm)	Average PDI	Average ZP (mV)
G300	253.16±15.5	0.071±0.013	24.59±1.6
G300PS100	252.26±27.8	0.11±0.035∗	20.33±5.1§
G300PS200	226.67±9.05♦	0.071±0.018	27.23±2.8
G275	83.43±23.0†	0.22±0.056	31.74±3.8
G275PS100	104.63±24.5	0.17±0.046	28.94±4.2‡
G275PS200	122.66±7.36	0.22±0.14	40.59±1.9

For the three Sigma Type A gelatin NP types, G300PS200 NPs were significantly smaller in diameter (∼226 nm) from either the G300 and G300PS100 NPs (∼253 nm), despite encapsulating a larger material (Table 2.1,♦ $p<0.05$)). The G300PS100 NP PDI was significantly higher than the G300 and G300PS200 PDI values (0.11 versus 0.071, respectively), reflecting a larger size distribution (∗ $p<0.05$). The G300PS100 ZP (∼20 mV) was statistically smaller than that of G300 (∼24 mV), indicating the particles were less positively charged when encapsulating the unmatched PS100 material (§ $p<0.05$).

For the three Vyse Type B NP types, the G275 NPs were significantly smaller in diameter (∼83 nm) from the G275PS200 NPs (∼122 nm) († $p<0.05$) and nearly significantly smaller from the G275PS100 NPs (∼104 nm) ($p = 0.08$), suggesting the addition of an encapsulation material increased the size of the gelatin type B NPs. None of the PDI values were significantly different for G275 (∼0.22), G275PS100 (∼0.17) or G275PS200 (∼0.22). G275PS100 was significantly smaller in ZP (∼28 mV) from G275 (∼31 mV) and G275PS200 (∼40 mV) (‡ $p<0.05$), suggesting these encapsulated G275PS100 particles are less stable.

2.4.2 Nanoparticle Stability

Once fabricated, the same batches were characterised over a 4-week period to determine stability of the NPs in distilled water (pH 3-4) at room temperature for storage conditions (Figure 1). For the purposes of this paper, stability is defined as insignificant changes in diameter, size distribution (PDI), or ZP. Overall, none of the NP types changed significantly in size or PDI over the 4-week period.

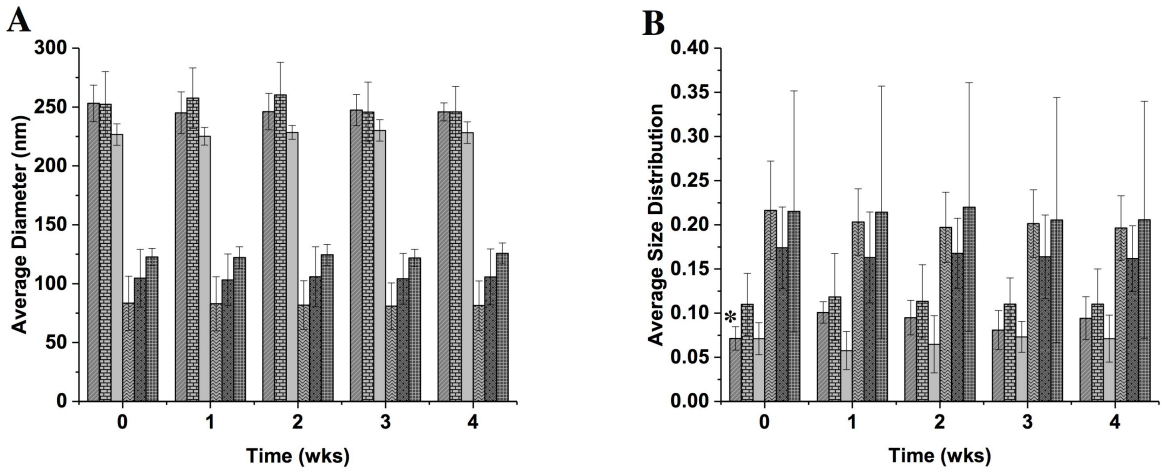

Figure 2.1: Changes in NP average diameter (A) and PDI (B) over time. NP types are designated as follows G300 (striped gray), G300PS100 (brick pattern), G300PS200 (solid gray), G275 (wave pattern), G275PS100 (dotted dark gray), and G275PS200 (crosshatch). (A) Changes in average diameter over 4 weeks for each NP type, (B) Changes in average NP PDI over 4 weeks for each NP type. Asterisks (*) indicate significant differences between samples ($p < 0.05$, $n = 3$)

As shown in Figure 2, the NP suspensions were cycled through one freeze/thaw in order to determine their stability under a standard storage condition. All of the NP types were able to survive the freeze/thaw cycle without significant changes in diameter or PDI.

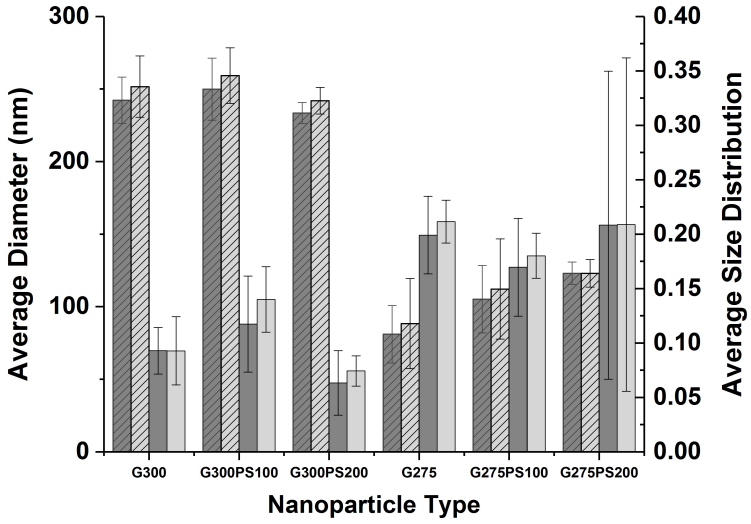

Figure 2.2: NP Stability Under Freeze/Thaw Conditions. Designations are as follows pre-freeze diameter (striped dark gray), post-freeze diameter (striped light gray), pre-freeze PDI (solid dark gray), and post-freeze PDI (solid light gray). (no significant differences between pre-freeze and post-freeze samples, n =3).

G300PS200 and G275PS100 were identified as the NP types with the preferred overall combination of initial average diameter close to the encapsulation material, initial average PDI between 0.1 and 0.2, and initial ZP close to +30 mV. These two matched NP types were further tested to determine stability over a physiological pH range of 1-9 during a 5-day-period. Both NP types had a baseline pH of 3-4 in distilled water prior to being adjusted to the desired pH values for the study.

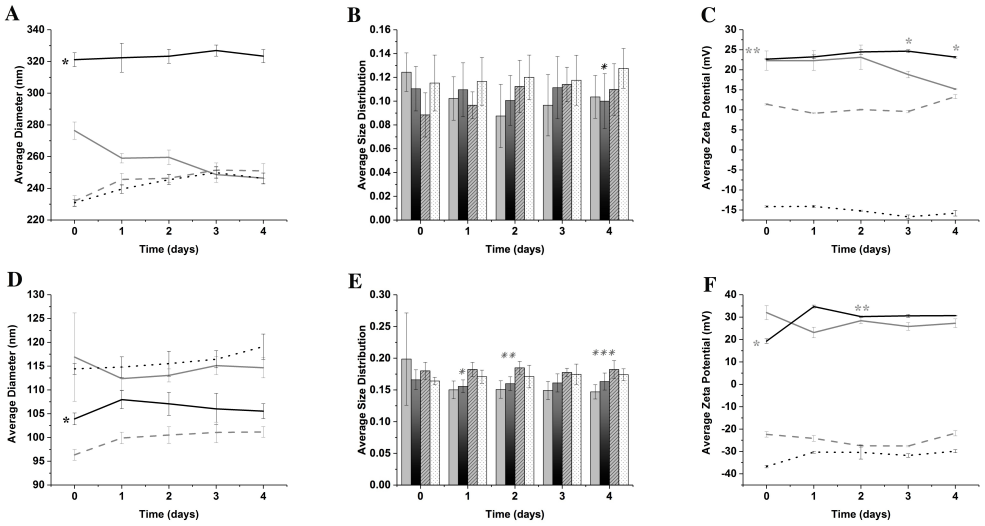

Figure 2.3: pH study of G300PS200 average diameter (A), average PDI (B) and average zeta potential (C); and G275PS100 average diameter (D), average PDI (E), and average zeta potential (F). Designations are as follow pH 1-2 (solid gray), baseline pH 3-4 (solid black), pH 5-6 (dashed gray), and pH 8-9 (dotted black). Asterisks (*,*,*,*) indicate significant differences between samples ($p<0.05$ and $n = 3$)

The average NP diameter, size distribution, and ZP for the G300PS200 NPs over a pH range of 1-9 are shown in Figure 3 A-C. The baseline pH 3-4 G300PS200 NP average diameter (Figure 3A, solid black line) was significantly larger in diameter throughout the 4-day-period than the G300PS200 diameters at the other pH values. (* indicate $p<0.05$). There were no significant changes in size distribution until day 4 where the baseline pH 3-4 size distribution (Figure 3B, black solid bar) was significantly smaller than the pH 8-9 size distribution (Figure 3B, black dotted bar), indicating instability at the higher pH range (* indicate $p<0.05$). The NPs also maintain a larger positive charge at pH 3-4 for days 0,1,2 (Figure 3C, black solid line), which is significantly larger than that of pH 5-6 (dashed gray line) and 8-9 (black dotted line). By days 3 and 4, pH 3-4 ZP is significantly larger than that of all the other pH values (* indicates $p<0.05$). The average NP diameter, PDI, and ZP for the G275PS100 NPs over a pH range of 1-9 are shown in Figure 3 D-F. The baseline pH 3-4 G275PS100 NP average diameter (Figure 3D, solid black line) was significantly larger in diameter than that of pH 5-6 and significantly smaller than that of pH 1-2 and pH 8-9 throughout the 4-day-period (* indicates $p<0.05$). The baseline pH 3-4 size distribution (Figure 3E, black solid bar) was significantly smaller than that of pH 5-6 and pH 8-9 (Figure 3E, dashed gray bar and black dotted bar,

respectively) for day 1 (* indicates $p<0.05$) significantly smaller than that of pH 5-6 (dashed gray line) for day 2 (** indicates $p<0.05$) and significantly different from that of pH 1-2 (solid gray line) and 5-6 (dashed gray line) for day 4 (*** indicates $p<0.05$). The NPs also maintain a significantly different positive charge at pH 3-4 for days 0,1,3,4 (Figure 3F, black solid line) than that of all of the other pH values (textcolorgray* $p<0.05$). On day 2, pH 3-4 ZP is significantly larger than that pH 5-6 (dashed gray line) and 8-9 (dotted black line) indicating storage in acidic conditions causes a strong positive NP charge (** indicates $p<0.05$).

2.4.3 Nanoparticle Imaging

TEM imaging was used to determine whether the NP suspensions contained unencapsulated beads, partially encapsulated beads, completely encapsulated beads or, as expected, a mixture of all three types; as well as to confirm the Zetasizer dynamic light scattering size range measurements from Tables 1 and 2. Figure 4 is a composite image of all NP types with insets showing the overall sample morphology. The expected range of NP sizes and types of encapsulation present were present, even with some coagulation artifact due to sample processing. The empty unencapsulated gelatin NPs were dark in colour with a large size range, scalloped edges, and porous morphology (barred black arrow) as shown in Figure 4 (A) and (D). The unencapsulated beads on TEM imaging were smooth edged and lightest in colour (Figure 4 outlined arrows (B) and (C)), the partially encapsulated NPs were intermediate in colour and still have fairly smooth edges (Figure 4 solid black arrows (B) and (C)), and the fully encapsulated beads were darkest in colour and have fuzzy edges (Figure 4 (E) and (F)). Additionally, a smaller size range was observed when the matched encapsulation material is used as shown in the TEM images of G300PS200 and G275PS100 in Figure 4 (C) and (E), respectively and the insets.

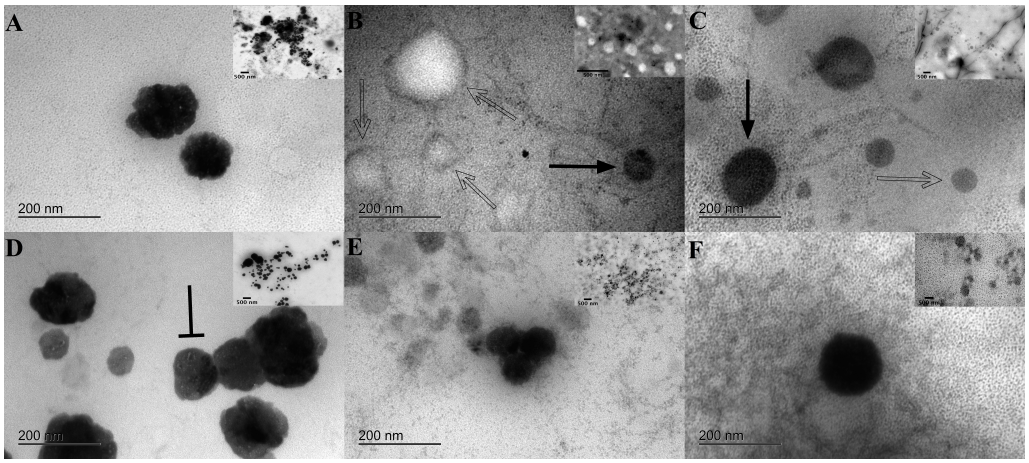

Figure 2.4: TEM Differences in Encapsulation Morphology for Nanoparticle Types. Designations are as follows (A) G300, (B) G300PS100, (C) G300PS200, (D) G275, (E) G275PS100, and (F) G275PS200. Outlined arrows indicate unencapsulated polystyrene beads. Solid black arrows indicate partially encapsulated polystyrene beads, and the barred arrow indicates an empty gelatin NP with evident porous morphology.

2.5 Discussion

Inclusion of an encapsulated material does affect the average diameter, size distribution, and ZP of the NPs (Table 2). When the material to be encapsulated was of similar size and shape to the empty NPs, the overall preferred combination of diameter, size distribution, and ZP was observed, as evidenced by the G300PS200 and G275PS100 encapsulated nanoparticles. The significant reduction in size observed with the matched G300PS200 NPs, despite having the larger encapsulation material, as well as the significantly higher size distribution seen with the unmatched G300PS100 NPs suggests that choosing an encapsulation material that closely matches the morphology of the empty gelatin NPs is a good strategy for controlling the fabrication process and leads to a 1:1 NP to encapsulation material ratio. This 1:1 ratio is further supported by the TEM results discussed below. Additionally, the matched material with its narrow distribution and ideal size parameters allows for consistency in NP in vitro release and cellular uptake studies. Using a material that does not match the size of the empty gelatin NPs led to more variation in encapsulation, causing a more variable average diameter, a larger average size distribution, and a more variable average ZP as seen with the G300PS100 and G275PS200 encapsulated nanoparticles types. Over time, this may lead to less

stable nanoparticles. The average size of the encapsulated G275PS200 NPs (∼122 nm) being smaller than the encapsulation material (200 nm polystyrene beads) can be attributed to the formulation including both partial encapsulations and empty encapsulations, leading to a smaller average size. Both G300PS100 and G275PS100 had the lowest ZP values, which may be due to the negatively charged PS1 particles having a wider size range than indicated by the manufacturer (and e.g. Figure 4B) leading to variation in the positively charged gelatin shell thickness and therefore a lower overall ZP [40, 32]. Regardless, all formulations had an average ZP sufficiently large enough to avoid aggregation or dissolution in suspension for the 4-week period as evidenced by the lack of significant changes in diameter and size distribution in Figure 1. In general, adding a matched encapsulation material appears to minimize the variation in the NP fabrication parameters compared to the empty NP fabrication results seen with G300 and G275. It was determined all NP batches were stable in distilled water (pH 3-4) at room temperature with regard to maintaining the same bulk average diameter and PDI up to 4 wk (Figure 1). For G300, the significant difference between the week 0 and week 1 PDI values can be attributed to residual acetone evaporation. In addition, each NP suspension was also put through a freeze/thaw cycle to determine if freezing was a viable option to potentially extend NP storage life. This test revealed that each NP type was able to endure a freeze/thaw cycle without significant changes to the average diameter or PDI. As the NPs can be frozen to extend the product lifespan prior to use, the results from Figure 1 and Figure 2 combined meet and exceed the production specification for the NPs to be stable in suspension at room temperature up to 1-month. When G300PS200 and G275PS100 were tested under varying pH conditions, pH 3-4 served as the baseline for comparison of average diameter, size distribution, and ZP. The significant differences seen in the study can be attributed to the effect of pH on polymer chain size within the NP and the surface charge. As the pH moves away from the gelatin polymer pI (Type A pI ∼pH 7-9; Type B pI ∼pH 4.7-5.4), the hydration state and charge of gelatin molecules will change. When the pH is above or below the pI, the polymer chains will swell or collapse thus increasing or decreasing the average NP diameter, respectively [9, 88, 1]. Concurrently, the charge on the gelation molecules will increase, leading to increased NP repulsion as the pH moves away from the gelatin's pI. For G300PS200, the diameter of the NPs was consistently larger at pH 3-4 compared to the other pH values over the 4-day-period. Polymer chain collapse leading to a decreased diameter is expected at pH 1-2, which is below the pI of Type A gelatin, even with high NP charge. The smaller sizes of the NPs at the pH values close to the Type A gelatin pI at pH 5-6 and 8-9 can be attributed to these being the least stable NPs due to having low surface charge, leading to NP falling apart. There were no significant differences in size distribution until day 4 when the pH 3-4 PDI was significantly smaller than that of pH 8-9. This suggests

that although the average diameter was significantly different over the entire 4-day-period, the overall spread of the NP sizes were similar for the first three days, but the effect of the higher pH eventually caused the pH 8-9 NPs to be more variable. A similar pattern where pH 3-4 is significantly different from both pH 5-6 and 8-9 is seen in Figure 3C as well. The pH 3-4 ZP is significantly different from pH 5-6 and 8-9 for days 0, 1, 2 and then significantly different from all pH values for days 3 and 4. Since pH 3-4 maintained the highest charge across all four days compared to the other pH values, this suggests that pH 5-6 and 8-9 are less stable due to the gelatin chains being less charged close to the Type A gelatin pI and that the NPs are able to survive in pH 1-2 for the first two days but eventually the acidic pH leads to a decrease in NP charge and then a decrease in average diameter as the NPs grow unstable and break apart. Ahsan and Rao's work contains a possible explanation as to the effect of pH on NP charge. Ahsan and Rao found the peak zeta potential values for Type A and Type B gelatin were pH 4 and 3.5, respectively. They hypothesized the increase in zeta potential in both gelatin Type A and Type B to a peak value of ∼20 mV in the pH range 3.5-4 is due to protonation of aspartic acid and glutamic acid. Lowering the pH below 3.5-4 lead to an unexpected decrease in zeta potential, which they potentially attributed to ion pair formation and Debye-Huckel screening [1]. For G275PS100, the diameter of the NPs was consistently smaller at pH 3-4 compared to pH 1-2 and 8-9 and larger than pH 5-6 over the 4-day-period. As the closest to the pI of the Type B gelatin (4.7-5.4), the pH 5-6 diameter values represent polymer chains that are neither swollen nor collapsed. It is expected that the polymer chains will be swollen above the Type B gelatin's pI at pH 8-9, leading to a larger diameter provided, as there is in this case, sufficient NP charge to avoid agglomeration. The pH 1-2 diameter is larger than expected base on the predicted polymer chain collapse below the gelatin pI but may be the product of a slightly lower zeta potential at the more acidic pH, leading to ion pair formation and Debye-Huckel screening as previously mentioned. For size distribution, the increased variability seen with pH 1-2, 5-6, and 8-9 suggests they are less stable over the 4-day-period compared to that of pH 3-4. For the ZP, all the pH values are close to either +30 mV or -30 mV, suggesting these NPs are more stable at different pH values due to Type B gelatin used. Our data agrees with Ahsan and Rao as the overall peak ZP values were found for both gelatin Type A and B at pH 3-4 and storage of the NPs in this pH range led to the preferred combination of average diameter close to the encapsulation material size, small size distribution, and large ZP over the four-day-period [25]. This indicated both NP types G300PS200 and G275PS100 were stable at pH 3-4 but begin to fall apart as the suspension pH approaches each gelatin's respective pI ranges or significant ion interactions come into play at extremely acidic or basic pH. The optimal storage pH for Type A and Type B gelatin NP suspensions was therefore at pH 3-4 and suggests the NPs would be ideal for

delivery in the body, where the acidic pH of the stomach or neutral pH of the blood would facilitate release of encapsulated material. The TEM imaging revealed that all three types of encapsulation were present in each NP sample and confirmed the DLS average size for each formulation (Table 2). The 1:1 NP to encapsulation material ratio should reduce the need for multiple filtration steps to achieve desired particle size range and PDIs, thus reducing the loss of encapsulated material during processing. All of these results taken together suggest matching the encapsulation material size to the initial empty gelatin NP size does result in a more uniform, stable particle for biological delivery.

2.6 Conclusions

The encapsulation system developed here demonstrates that different NP types can be consistently produced to meet desired specifications with matched encapsulation material NPs having the preferred overall parameters. This proves the encapsulation system is customizable to encapsulating different nanometer sized materials and were stable both at room temperature and after freeze/thaw conditions for storage. The encapsulation system is most stable at pH 3-4 but begins to fall apart outside that pH range. This system shows promise for being easily adaptable for sustained delivery of biologics to patients due to the multiple types of encapsulation present in each formulation. While we have used a stable particle stand-in for initial fabrication and characterisation of the basic encapsulation system, the next step will be to modify the system for different biomedical applications. Future studies include encapsulating spherical biologics such as viruses to determine their characteristic NP profiles and release profiles; lyophilization of different NP formulations to determine if an alternative dry formulation can be created; modification of the reactive groups on the gelatin polymer encapsulation shell for targeting purposes; and studying NP uptake and cytotoxicity for the cell populations of interest given different biomedical applications.

2.7 Acknowledgements

Authors would like to thank the VT Regenerative Medicine Interdisciplinary Graduate Education Program (IGEP) and the VT Biomedical Engineering and Mechanics Department for support, the Virginia-Maryland College of Veterinary Medicine Morphology Lab for their expertise with TEM imaging, and André Stevenson, Jr. for his expertise on the double desolvation method for NP fabrication.

Chapter 3

Cellular In Vitro Effects of Gelatin-Chitosan Nanoparticle Vaccine Delivery on Turkey Lymphoblastoid Cells and Chicken Fibroblasts

This paper will be submitted to *Vaccine*. The work shown encompasses Aims 2 and 3.

3.1 Abstract

Development of new vaccine delivery technology has been limited due to a lack of adjuvants available to non-injectable methods. Our hypothesis was that using gelatin and chitosan as polymeric adjuvants in killed virus vaccine formulations would enable oral delivery. As a step towards *in vivo* testing, virus encapsulated

in gelatin-chitosan nanoparticles (NPs) was tested in cell populations of interest *in vitro* for uptake and normal cell growth and viability. Hemorrhagic enteritis virus (HEV) and fowlpox virus (FPV) were chosen as the viruses for proof-of-concept as these are poultry viruses of economic impact [83]. Real-time qPCR with design of experiment (DOE), dynamic light scattering (DLS) analysis and transmission electron microscopy (TEM) were used to characterize the viral vaccine formulations. The vaccine formulations was tested in representative cell lines to ensure the viral nanoparticles could be viably taken up and tolerated by the cell lines of interest in addition to empty gelatin-chitosan NPs. Confocal microscopy was used to confirm uptake within 1 hr by the cell populations of interest. Lactose dehydrogenase (LDH) assay found the HEV-GC NP formulation induced significant cytotoxicity, which may be beneficial in stimulating protective immunity. However, CellTiter 96 AQ_{ueous} One Solution Cell Proliferation (MTS) Assay demonstrated that both cell lines were viable over a 7-day-period in the presence of NPs, suggesting the cytotoxicity induced through killed virus nanoparticle treatment does not lead to cell death. These combined results demonstrate cellular uptake and safety of the killed virus formulations prior to clinical and challenge studies to determine nanovaccine formulation efficacy, safety in poultry, and ability to protect in the face of live virus challenge.

3.2 Introduction

Next generation vaccines will only be possible when new adjuvants are found to enable non-injectable delivery methods [65]. Gelatin and chitosan are our proposed adjuvants for oral delivery of killed virus vaccines. Both are natural polymers already in clinical use and have the reported ability in scientific literature to enhance delivery of associated antigens [31, 40, 27, 28, 32, 69, 41, 19, 51, 6, 11, 42, 44, 10, 50, 68]. The Food and Drug Administration (FDA) has classified gelatin as 'Generally Recognized as Safe' excipient and gelatin is biodegradable without production of toxic breakdown products. It has been shown to target antigens to dendritic cells which may lead to activation and priming of T cells, has opsonic abilities for macrophage phagocytosis, and can be used with the two-step desolvation technique to produce simple and reproducible particles [81, 94, 61]. Chitosan is a known mucoadhesive derived from shellfish, which has been used as dietary fiber as well as in various pharmaceutical applications. It is able to increase the bioavailability of various compounds including vaccines through adhesion to the mucosa and enhancing absorption. Chitosan is also able to open cellular tight junctions to improve transport of antigens [11, 42, 82]. It has been reported to enhance both systemic and cellular immune responses with mucosal delivery [44, 42, 39, 82]. These

combined properties make gelatin and chitosan promising as oral adjuvants in a killed virus delivery system. Turkey hemorrhagic enteritis virus (HEV) and chicken fowlpox virus (FPV) have been chosen as viruses of economic importance in poultry for encapsulation in initial nanoparticle vaccine formulations [83]. Using killed virus in the formulations improved vaccine safety through avoiding the cytopathic effects of the live viruses replicating in cells. Our hypothesis was that the viral gelatin-chitosan NP formulations would be able to be successfully fabricated, uptaken by the target cell lines, and tolerated with normal cell growth over a 7-day period. These cell studies were used as a check for cellular uptake and safety of the the nanoparticle formulations prior to *in-vivo* studies.

3.3 Materials and Methods

Type A 300 Bloom gelatin (Sigma-Aldrich; St. Louis, MO) was used to encapsulate the two viruses of interest in the two step desolvation NP fabrication process. Commercially available HEV and FPV propagated through MDTC-RP19 (ATCC CRL-8135^{TM}) turkey lymphoblastoid and UMNSAH/DF-1 (ATCC CRL-12203^{TM}) chicken fibroblast cell lines respectively, were used as encapsulation materials. MDTC-RP19 cells were cultured under standard conditions as previously described. Briefly, MDTC-RP19 cells were maintained in complete RP19 media and HEV was added to approximately 500,000 cells and incubated until the cytopathic lysis effect was seen in the majority of cells at which point, the culture was centrifuged and the supernatant containing the HEV harvested [52]. UMNSAH/DF-1 cells were cultured using the standard ATCC protocol until a monolayer formed in approximately 2-3 days. FPV was added to the monolayer and incubated until the majority of cells were lysed at which point, the culture was centrifuged and the supernatant containing the FPV harvested [84]. Low-molecular weight chitosan (Sigma-Aldrich; St. Louis, MO) was used to coat the gelatin and stabilize the nanoparticles in solution. Lactose dehydrogenase (LDH) assay (Thermofisher Scientific; High Point, NC) and CellTiter 96 AQ_{ueous} One Solution Cell Proliferation (MTS) Assay (Promega; Madison, WI). All other materials were analytical grade and used as received.

3.3.1 Nanoparticle Preparation

A two-step desolvation method was used to make empty (GC) and viral-encapsulated nanoparticles (HEV-GC or FPV-GC) as previously described [20, 80] . HEV and FPV were replicated in their respective cell

lines as previously described [52, 18] but with fetal bovine serum increased to 15% for the chicken fibroblasts in order to achieve normal growth. Supernatants were collected and then diluted to yield $9.50E+04$ virions of HEV and $1.45E+07$ virions of FPV for use in each respective NP batch. These amounts of virus were determined to yield viral particle formulations with consistent DLS characteristics for use in cell studies.

3.3.2 Real-time PCR and Design of Experiment Array

In order to determine the set of fixation parameters to ensure HEV could not replicate but still could be detected using real-time polymerase chain reaction (q-PCR), a design of experiment (DOE) array was performed. Fixation temperatures of 4^oC or 25^oC; 0.02, 0.1, or 0.25 % fixative amount; and fixation times of 3, 6 or 24 hr were tested in the array. JMP Pro Software's Prediction Profiler found the amount of HEV detected through qPCR DNA detection was maximized when the virus was fixed with 0.02 % paraformaldehyde at 4^oC for 6 hr (data not shown). To determine if the fixed virus could replicate, equal amounts of fixed and unfixed HEV ($9.50E+04$) were incubated with MDTC-RP19 turkey lymphoblastoid cells for 8 days prior to supernatant harvesting for qPCR analysis as previously described[52]. The unfixed HEV was able to replicate and the number of virions detected increased ($2.13E+06$) while the number of virions for the fixed HEV was found to be ($1.69E+03$), indicating the fixed virus was unable to replicate but still detectable. The same fixation conditions were used for FPV fixation prior to nanoparticle encapsulation.

3.3.3 Virus and NP Characterization

The double desolvation method was used to fabricate the NPs as previously described [20, 80]. Dynamic light scattering was used to obtain the basic characteristics of each fixed virus and NP type. An aliquot of the sample suspension (100 µL) was diluted into deionized water (900 µL) in a plastic cuvette and three measurements were taken to estimate the average diameter and size distribution of each sample using cumulants analysis with a Zetasizer- Nano-ZS (Malvern instruments; Southborough, UK). The remainder of the sample suspension was stored at room temperature in 50 mL plastic conicals.

3.3.4 NP Purification

NP suspensions were centrifuged at 12,000 rpm and 25^{o}C for 5 min to concentrate them. The supernatant was decanted and the pellet washed three times with 5 mL phosphate buffer saline. The pellet was vortexed until resuspended in 5 mL phosphate buffer saline (PBS) and then 0.22 micron or 0.45 micron filtered to make a total of 5 mL of NP sterile suspension prior to cell studies.

3.3.5 NP Morphology TEM Imaging

Each cell line (1 million cells) was exposed to NPs (600 µL) for 1 hr, then fixed with an equal volume of Karnovsky's fixative for 24 hr. The fixed cell-NP suspensions were dehydrated in 100 % ethanol for 4 hr, filtered onto a nanocellulose membrane, and dried with a LADD critical point dryer overnight. The NPs were stained with lead citrate prior to imaging with a JEOL JEM-1400 Transmission Electron Microscope (JEOL Ltd.; Akishima,Japan).

3.3.6 Cellular Uptake Confocal Imaging

Live confocal microscopy imaging was used to determine NP uptake by each respective cell line. Briefly, cells (500,000) were seeded onto glass slips and allowed to attach overnight for the chicken fibroblasts. NP suspensions were added to the glass slips (200 µL) with the appropriate complete media (300 µL) and incubated for 1 hr. NucBlue dye was used to stain cellular nuclei to aid sample visualisation for 15 min and then cells were washed once with PBS prior to imaging with a Zeiss LSM 800 (Zeiss; Oberkochen, Germany).

3.3.7 LDH Cell Assay

For both cell lines, cells were seeded in triplicate wells in a 96 well plate (5,000 cells/well). Either empty GC or viral GC NPs were introduced to each well at either 10% or 0.1% total volume. The turkey lymphoblastoid cells were incubated for 1 hr prior while the chicken fibroblasts were incubated for 24 hr prior to LDH assay to determine the chemical cytotoxicity of the NP treatments.

3.3.8 MTS Cell Assay

Turkey lymphoblastoid cells (50,000) were seeded in duplicate wells in six 6 well plates in media (2 mL). Either treatment, empty GC or viral GC NPs were introduced to each well at either 0.5% (low dose) or 5% (high dose) total volume with untreated cells as a control. The contents of each well were centrifuged at 12,000 rpm for 7 min at 5°C in 15 mL conicals and the cell pellets were resuspended in fresh media and given fresh NP treatments every 3 days as described before. The turkey lymphoblastoid cells were incubated at 39°C with 5% CO_2, for 1, 3 or 7 days prior centrifugation and movement of cell suspensions to 96 well plates for MTS assay with a Spectramax 340PC Microplate Reader (Molecular Devices; Sunnyvale, CA) to determine the cell viability with NP treatment.

Chicken fibroblasts were seeded in triplicate wells in three 96 well plate (5,000 cells/well) and allowed to attach overnight in media (200 µL). Empty GC or viral GC NPs were introduced to each well at either 0.5% (low dose) or 5% (high dose) total volume with untreated cells as a control. The supernatant was removed from each well and fresh media and treatments were given as described before every two days. The chicken fibroblasts were incubated for 1, 4 or 7 days at 41°C with 5% CO_2 prior to MTS assay with a Spectramax 340PC Microplate Reader (Molecular Devices; Sunnyvale, CA) to determine the cell viability with NP treatment.

3.3.9 Statistical Analysis

One-way ANOVA analysis was used to determine whether significant differences existed between sample groups. When significance was present, Tukey's HSD Test was used to reveal which samples were significantly different. JMP Pro Software (v. 12.0.1, SAS Institute Inc., Cary, NC) was used for all statistical analysis. Data are reported as averages ± standard error with three replicates.

3.4 Results

Prior to encapsulation, dynamic light scattering was used to obtain the basic properties of the HEV and FPV as shown in Table 3.1.

Table 3.1: Properties of HEV and FPV. One sample was measured three times for each virus and values are reported as the average ± standard deviation. (n = 3 measurements).

Virus	Average Diameter (nm)	Average Size Distribution
HEV	87.56±1.49	0.57±0.004
FPV	171.67±1.33	0.53±0.008

The viruses were separately fixed with 0.02% paraformaldehyde for 6 hrs at 4°C, which was the optimal fixation protocol determined through a design of experiment array. The viruses were then encapsulated in gelatin-chitosan nanoparticles using the double desolvation fabrication method. Data are shown below in Table 3.2.

Table 3.2: Empty gelatin-chitosan (GC), hemorrhagic enteritis virus encapsulated gelatin-chitosan (HEV-GC), and fowlpox encapsulated gelatin-chitosan (FPV-GC) nanoparticle average diameter and size distribution before and after purification measured using DLS. Each NP fabrication type was centrifuged, washed three times with PBS, resuspended in PBS, and 0.22 or 0.45 micron filtered for purification. Data are reported as average ± standard deviation (n = 3).

Nanoparticle Type	Average Diameter (nm)	Average Size Distribution
GC	396.58±94.98	0.31±0.05
Purified GC	207.00±33.99	0.38±0.15
HEV-GC	299.73±33.03	0.17±0.06
Purified HEV-GC	202.76±23.78	0.11±0.03
FPV-GC	323.90±13.75	0.21±0.03
Purified FPV-GC	340.13±77.50	0.56±0.16

Suspected HEV-GC NP morphology using confocal microscopy as seen in Figure 3.1.

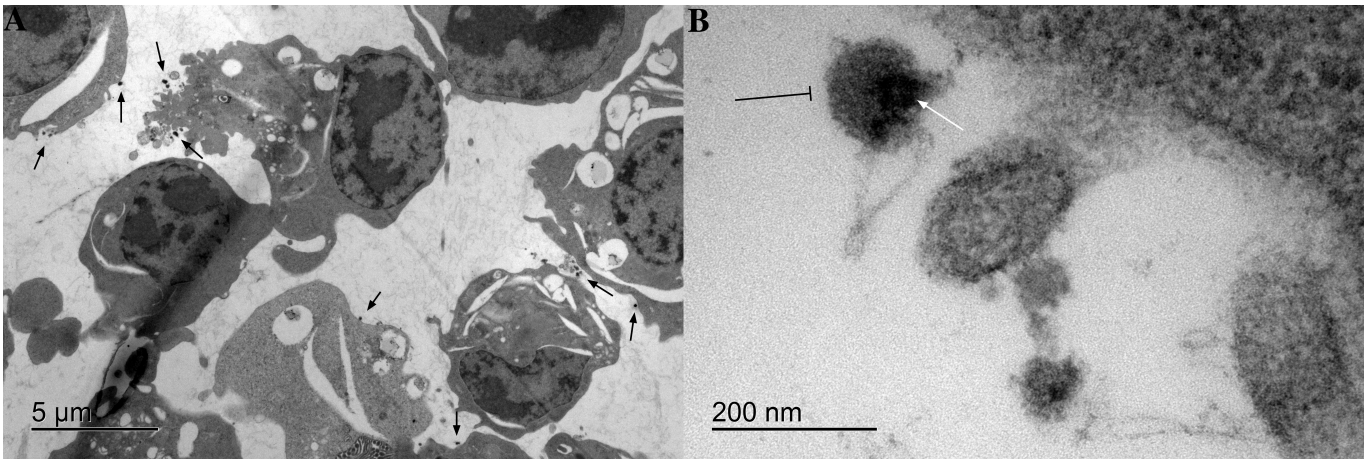

Figure 3.1: Representative TEM of MDTC-RP19 turkey lymphoblastoid cells exposed to HEV-GC NPs. (A) Overview image with suspected HEV-GC NPs denoted with black arrows on cell peripheries (B) Opened nanoparticle (barred arrow) with 70-90 nm HEV (white arrow) inside. These images suggest the turkey lymphoblastoid cells are able to tolerate HEV-GC NPs (B) and that HEV was successfully encapsulated in the gelatin-chitosan NPs (B)

Suspected FPV-GC NP morphology using confocal microscopy seen in Figure 3.2.

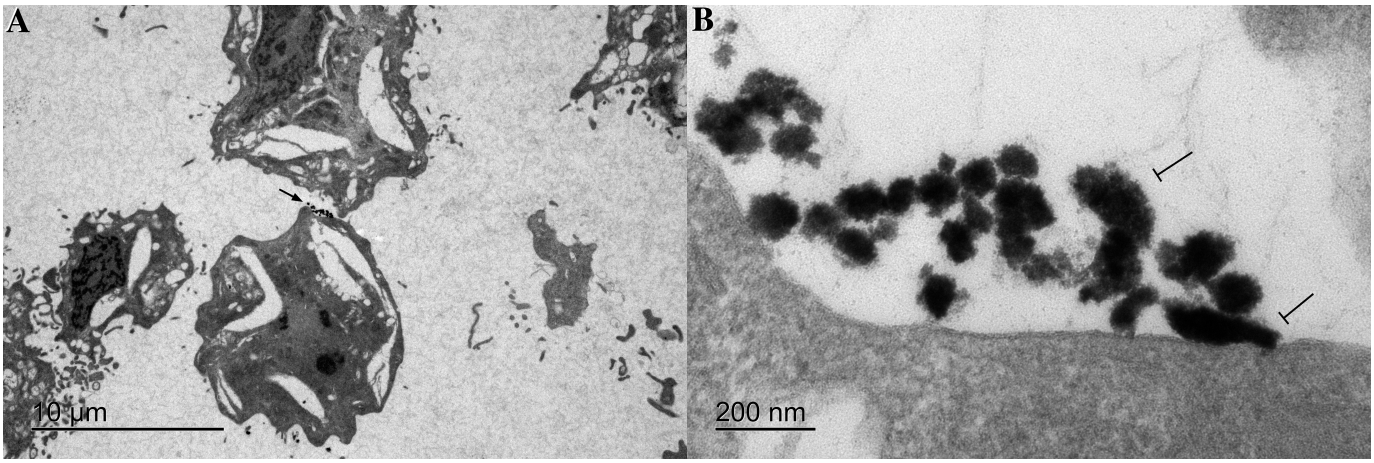

Figure 3.2: Representative TEM of UMNSAH/DF-1 chicken fibroblast cells exposed to FPV-GC NPs. (A) Overview image in which the black arrow outlines a cluster of potential FPV GC NPs on the cellular periphery. (B) Nanoparticle cluster where the barred arrows show FPV-GC NPs that match expected viral NP dimensions. Remaining NPs may be end on view of the viral NPs or empty GC NPs.

Uptake of GC and HEV-GC nanoparticle types in RP19 turkey lymphoblastoid cells was confirmed using confocal microscopy as seen in Figure 3.3.

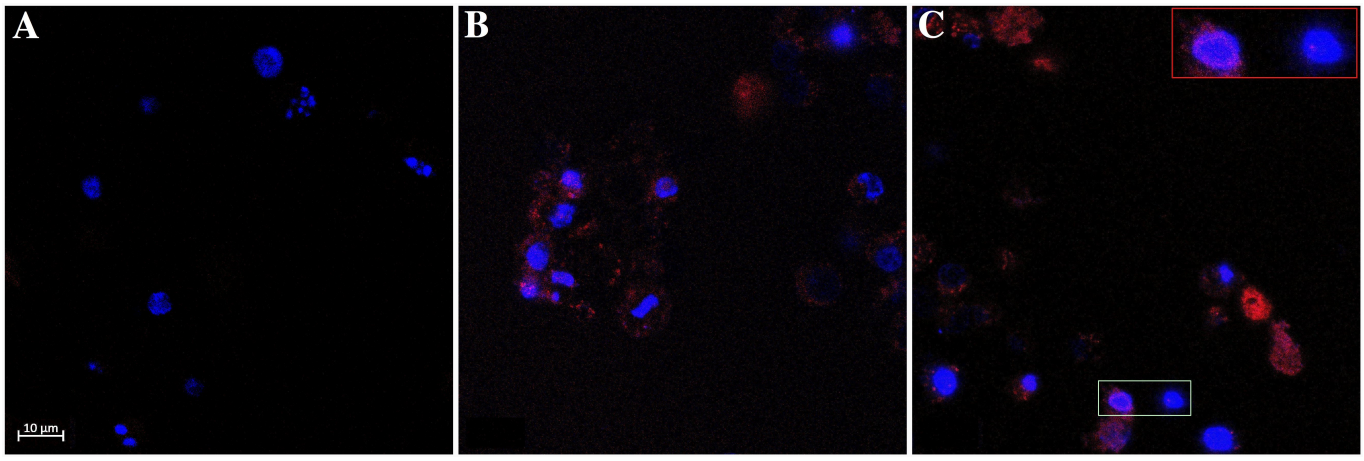

Figure 3.3: Cellular Uptake of Autofluorescent Nanoparticles in MDTC-RP19 Cells. Designations are as follows (A) Plain RP19 cells, (B) Gelatin-chitosan nanoparticles, (C) HEV-encapsulated gelatin-chitosan nanoparticles. NucBlue dye was used to stain live RP19 cell nuclei blue for contrast. The inset in part (C) at 2x zoom (red box) compares two RP19 nuclei (green box) and shows clustering of autofluorescent nanoparticles around one cell nucleus.

Uptake of GC and FPV-GC nanoparticle types in UMNSAH/DF-1chicken fibroblasts was confirmed using confocal microscopy as seen in Figure 3.4.

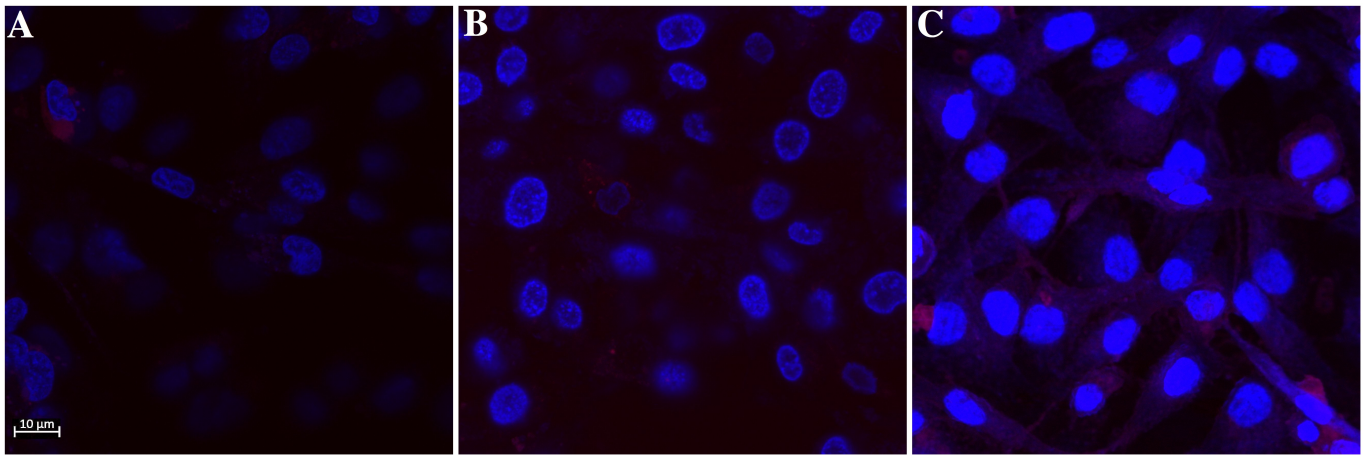

Figure 3.4: Cellular Uptake of Autofluorescent Nanoparticles in UMNSAH/DF-1 Cells. Designations are as follows (A) Plain UMNSAH-DF1 cells, (B) Gelatin-chitosan nanoparticles, (C) FPV-encapsulated gelatin-chitosan nanoparticles. NucBlue dye was used to stain live UMNSAH/DF-1 cell nuclei blue for contrast.

For the LDH assay, the 10% GC NP and HEV GC 10 % treated lymphoblastoid cells with an incubation time of 1 hr had 3.74 % and 33.02 % chemical cytotoxicity, respectively. The 10 %GC NP and 0.1 %FPV GC treated fibroblasts with an incubation time of 24 hr had 2.24 % and 2.81 % chemical cytotoxicity, respectively. The chemical cytotoxicity measured in this assay is indicative of LDH release from plasma cell membrane damage All other combinations had negative chemical cytotoxicity, which was corrected to zero.

MDTC-RP19 Turkey lymphoblastoid cell viability with different nanoparticle treatments was compared over a 7-day-period. The results are seen below in Figure 3.5.

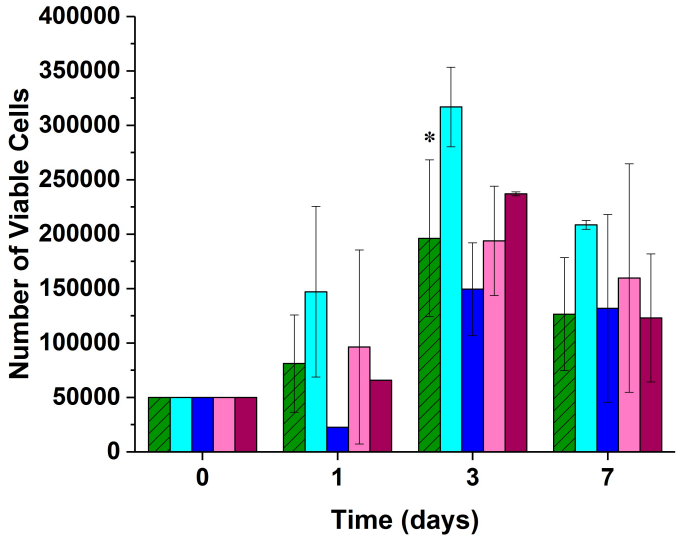

Figure 3.5: RP19 cell viability over time. Designations are as follows: untreated (green striped), low dose gelatin-chitosan nanoparticle treatment (light blue), high dose gelatin-chitosan nanoparticle treatment (dark blue), low dose HEV-encapsulated gelatin-chitosan nanoparticle treatment (pink), and high dose HEV-encapsulated gelatin-chitosan nanoparticle treatment (dark pink). Asterisk (*) designates significant differences ($n = 3$, $p<0.05$). RP19 cells treated with nanoparticles were not significantly different from untreated control apart from day 4 where the untreated control (green striped) is significantly lower than the low dose gelatin-chitosan nanoparticle treatment (light blue).

UMNSAH/DF-1chicken fibroblast cell viability with different nanoparticle treatments was compared over a 7-day-period. The results are seen below in Figure 3.6.

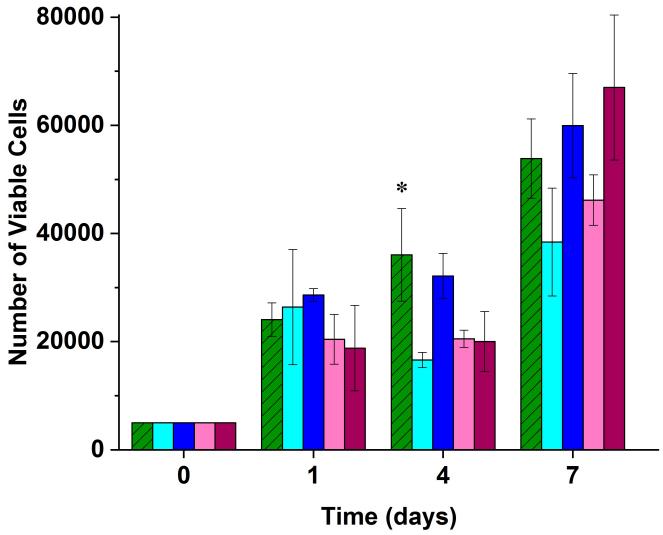

Figure 3.6: UMNSAH/DF-1 cell viability over time. Designations are as follows: untreated (green striped), low dose gelatin-chitosan nanoparticle treatment (light blue), high dose gelatin-chitosan nanoparticle treatment (dark blue), low dose FPV-encapsulated gelatin-chitosan nanoparticle treatment (pink), and high dose HEV-encapsulated gelatin-chitosan nanoparticle treatment (dark pink). Asterisk (*) designates significant differences (n = 3, $p<0.05$). UMNSAH/DF-1 cells treated with nanoparticles were not significantly different from the untreated control apart from day 4 where the untreated control (green striped) is significantly higher than the low dose gelatin-chitosan nanoparticle treatment (light blue) and both FPV nanoparticle treatments (pink and dark pink).

3.5 Discussion

The initial fixed virus average diameter and size distribution (Table 3.1) was measured in order to provide a benchmark for the nanovaccine encapsulations (Table 3.2). From these two tables, it can be clearly seen the particle average diameter increases from the plain HEV virus (87.56 nm) to the unpurified HEV-GC NPs (299.73 nm) and when purified, a decrease in average diameter to (202.76 nm). A similar trend is seen for the FPV virus (171.67 nm) to encapsulated NPs with the exception that the unpurified FPV GC NPs (323.90 nm) are slightly smaller than the purified FPV GC NPs (340.13 nm). The HEV virus is an icosahedral shape,

which yields more accurate results for DLS analysis that assumes a spherical particle shape. Because the FPV virus is a brick-shaped virus and not spherical, the DLS results are not as accurate but still serve as a useful basic check to ensure an increase in average diameter is seen with encapsulation in NPs. As shown in previous work, including an encapsulation material like the HEV virus does improve the consistency of the NP formulation in terms of an average diameter close to the encapsulation material diameter and a smaller size distribution as compared to the empty GC NPs.

TEM was used to determine the morphology of the viral NPs associated with each cell line (Figure 3.1 and 3.2) and confirm the DLS parameters (Table 3.2). For the HEV-GC NPs, a NP is evident in which a polymer coating (barred arrow) surrounds a suspected dark virion (white arrow) matching the known HEV dimensions (70-90 nm diameter, icosahedral shape) [13,15]. The spherical HEV-GC NPs are found in close association with the turkey lymphoblastoid cells (Figure 3.1, black arrows), but the NPs could not be positively identified within the cells to confirm uptake. Likewise, for the FPV-GC NPs, polymer-coated brick-shaped NPs are seen (Figure 3.2, barred arrows) in close association with the chicken fibroblasts (Figure 3.2, black arrow). The overall FPV-GC NPs diameter correlates with the DLS average diameter (Table 3.1).

DLS and TEM served to characterize and confirm the empty GC, HEV-GC and FPV-GC NP formulations were successfully fabricated. In order to determine if each NP type could be taken up by the cell populations of interest, fluorescent confocal microscopy was performed (Figures 3.3 and 3.4). The NP formulations were found to autofluoresce (red) while NucBlue dye was used to stain cell nuclei (blue). The autofluorescence is an attribute of gelatin and thought to be due to pentosidine crosslinks between arginine and lysine. Red fluorescence from the NPs increases from the plain cells (Figures 3.3 and 3.4 (A)) to the GC NP treated cells Figures 3.3 and 3.4 (B)) to the viral NP treated cells (Figures 3.3 and 3.4 (C)). This supports the TEM finding that the viral NPs are found in association with each cell line and further demonstrates each cell line is able to uptake its respective viral NP within 1 hr of exposure.

The LDH assay demonstrated the NP formulations, even dosed at the higher 10 % volume elicited minimal chemical cytotoxicity in each cell line ($\sim$ 2-3 %) with the exception of the HEV-GC 10 % dose, which elicited a surprising amount of chemical cytotoxicity ($\sim$33 %). This result warranted further investigation as vaccine adjuvants may act as depots or induce inflammation in order to stimulate the body to respond to delivered antigen. However, an adjuvant that elicits an overwhelming inflammatory response can lead to adverse effects or even death [61, 15, 79].

In order to determine whether each cell line could grow and remain viable in the presence of NP treatment, MTS assay was performed. For the RP19 turkey lymphoblastoid cells, neither the low (Figure 3.5, pink) nor high dose (Figure 3.5, dark pink) HEV-GC NP treated cells were significantly different from the untreated control cells (Figure 3.5, green striped) over the 7 day period. This suggests that the amount of chemical cytotoxicity elicited by the HEV-GC NPs measured in the LDH assay over a shorter time period of hours does not significantly affect the cells' viability over a longer time period of days. A similar trend was found for the FPV-GC NP treated chicken fibroblasts (Figure 3.6).

3.6 Conclusions

In this work, HEV and FPV were used as encapsulation materials in two killed virus nanovaccines with gelatin and chitosan as polymeric adjuvants. Viral NP fabrication and cell studies were performed as necessary steps prior to in vivo experiments. DLS and TEM showed both viruses were encapsulated in gelatin-chitosan NPs with the expected average diameters and size distribution. Confocal microscopy demonstrated viral NP uptake within 1 hr for both viruses in their respective cell lines. LDH assay found the HEV-GC NP formulation induced significant chemical cytotoxicity in turkey lymphoblastoid cells. For vaccine formulation, compounds capable of inducing a significant but not overwhelming inflammatory reaction are often potent adjuvants capable of inducing protective humoral or cellular immunity[66]. The HEV-GC NP formulation chemical cytotoxicity result /textitin vitro may translate to a HEV-GC NP vaccine formulation being able to induce inflammation on in *in viv* level suitable for induction of immunity. MTS showed that both cell lines were viable over a 7-day-period in the presence of nanoparticles, suggesting any chemical cytotoxicity induced through killed virus nanoparticle treatment is not overwhelming *in vivo*. These results combined demonstrate the safety of the killed virus formulations and that the target cells are able to uptake and grow in the presence of the nanovaccine. Next steps include performing proof of concept in animal studies to determine nanovaccine formulation efficacy, safety in poultry, and ability to protect in the face of challenge.

3.7 Acknowledgements

Authors would like to thank USDA NIFA Fellows Program (2018-67011-28039), VT Regenerative Medicine Interdisciplinary Graduate Education Program (IGEP), and the VT Biomedical Engineering and Mechanics

Department for support;the Virginia-Maryland College of Veterinary Medicine Morphology Lab for their expertise with TEM imaging; Amanda Covey, Nancy Tenpenny, Brittany Mehrkens, and Amanda Kravitz for support and advice.

Chapter 4

Immunological Efficacy of Gelatin Chitosan Adjuvanted Vaccine Delivery in Turkeys

This paper will be submitted to *Vaccine*. The work shown encompasses Aim 4.

4.1 Abstract

The field of vaccine technology is limited in delivery methods due to a lack of adjuvants available to enable different methods. Discovery of new adjuvants would move next generation vaccine development forward, allowing conversion of injectable vaccines to oral, nasal, and topical vaccines. Our hypothesis was gelatin and chitosan as polymeric adjuvants in a killed virus vaccine formulation would enable water-based delivery in turkeys to induce protective immunity. Hemorrhagic enteritis virus (HEV) was chosen for proof-of-concept prior to conversion of injectable vaccines to oral delivery. Killed HEV was encapsulated in a gelatin-chitosan nanoparticle as a nanovaccine and in a second vaccine formulation with loose gelatin and chitosan polymers (no nanoparticle). Real-time polymerase chain reaction (qPCR) confirmed the paraformaldehyde

was able to kill the HEV prior addition to the vaccine formulations. The killed HEV nanovaccine was able to induce cellular immunity and protect the turkeys from challenge with live HEV based on body-to-spleen ratios, splenic qPCR for viral clearance, and histopathology. By comparison, the killed HEV with loose polymers vaccine formulation was able to induce both humoral and cellular immunity as well as protect from live HEV challenge as measured by serum antibody titers and the aforementioned analyses. This work demonstrates the ability of gelatin and chitosan to act as oral polymeric adjuvants to stimulate protective immunity with killed HEV. The killed HEV with loose gelatin and chitosan was ultimately the more consistent formulation as compared to the killed HEV nanovaccine in the following benchmarks of immunity: antibody development within the 3-week time period post-vaccination, clearance of live HEV challenge as measured with qPCR, and the histopathology germinal centers count. This suggests gelatin and chitosan do not need to encapsulate the whole virus antigen in order to act as adjuvants in the formulation and simplifies the vaccine fabrication process significantly. The discovery of paraformaldehyde's ability to kill virus while preserving viral morphology for immune recognition and gelatin and chitosan's abilities to act as adjuvants in killed virus oral delivery formulations will move the field of vaccine development forward to allow conversion of injectable vaccines to oral vaccines across species.

4.2 Introduction

Development of next generation vaccines has been limited due to a lack of adjuvants to enable non-injectable delivery methods. The most common adjuvant is still alum salts, which has been in wide use for the past 70 years. Its method of action is attributed to depot effects in which the alum attracts immune cells to itself and associated vaccine antigen as well as induced inflammation. However, these effects can be detrimental to fatal when alum is delivered in any non-injectable form [61, 15, 79]. Therefore, new adjuvants must be tested in order to determine their safety, efficacy, and ability to enable other delivery methods. This work seeks to test gelatin and chitosan as polymer adjuvants to enable oral vaccine delivery in turkeys. Our hypothesis was gelatin and chitosan would enhance viral antigen uptake during oral delivery and stimulate protective immunity. Gelatin is a natural polymer derived from collagen, generally recognized as safe (GRAS-certified) by the FDA, and has a long history of safe use in pharmaceuticals, cosmetics, and food products [20,29-35]. As an adjuvant, gelatin enhances uptake of nanoparticles and the immunostimulatory ability of encapsulated antigen, specifically via upregulation of MHC II and CD86 molecules on dendritic cell surfaces leading to

more T cell activation and priming [94, 81]. Gelatin is also reported to have an opsonic ability for macrophage phagocytosis, meaning the gelatin facilitates delivery of a large amount of antigen to macrophages which then are stimulated and cause increased secretion of lymphokines and nonspecific cytotoxicity [61]. Chitosan is a cationic polysaccharide derived from shellfish chitin extract. Due to the protonated amino groups, chitosan is cationic and has adhesive properties for anionic surfaces, including mucus and proteins. Chitosan has been used to enhance oral and nasal delivery of antibiotics, antihypertensive agents, DNA, peptide drugs, vaccines and proteins [69, 41, 19, 51, 6, 11, 42, 44, 10, 50, 68] . The not fully elucidated mechanism is believed to involve enhanced uptake from transient opening of intercellular tight junctions, which both improves uptake of macromolecules and slows mucociliary clearance to increase the bioavailability of the delivered antigen [69, 93, 19, 6, 11, 10, 50]. Turkey hemorrhagic enteritis virus (HEV) was chosen for proof-of-concept because it is a virus of economic interest in the poultry industry and has water-based delivery live virus vaccines already commercially available, making it useful to test a new water-based delivery system with killed virus prior to converting injectable vaccines [83].

4.3 Materials and Methods

Avirulent hemorrhagic enteritis virus (HEV) propagated in MDTC-RP19 (ATCC CRL-8135$^{\text{TM}}$) turkey lymphoblastoid cells were used with Type A 300 Bloom gelatin (Sigma-Aldrich; St. Louis, MO) and low-molecular weight chitosan (Sigma-Aldrich; St. Louis, MO) as polymeric adjuvants for oral vaccination. All other materials were analytical grade and used as received. A power analysis was performed using literature data on spleen-to-body ratio to estimate the number of turkeys required for the clinical study [64].

4.3.1 Vaccine Preparation and Characterization

HEV propagated in MDTC-RP19 turkey lymphoblastoid cells was used for all viral treatments at a dose of $9.50E+04$ as measured with qPCR (data not shown) in (500 µL) serum-reduced complete MDTC-RP19 media aliquots as previously described[52, 64]. The double desolvation method was used to fabricate the GC and HEV-GC nanovaccine NPs as previously described [20, 80]. For the HEV-GC nanovaccine, HEV was fixed with 0.02% paraformaldehyde at 25^{o}C for 6 hr to kill the virus but preserve its morphology. The HEV with polymers treatment consisted of the fixed HEV in mixed with 0.02 g each of gelatin and chitosan

polymers loose in solution (no nanoparticle), sterile 0.22 micron filtered with phosphate buffer saline (5 mL), frozen at -20^oC, and then lyophilized.

GC or HEV-GC nanovaccine NP suspensions were concentration by centrifugation at 12,000 rpm and 25^oC for 5 min. The supernatant was decanted and the pellet washed three times with 5 mL phosphate buffer saline. The pellet was vortexed until resuspended in 5 mL phosphate buffer saline (PBS) and then 0.22 micron filtered prior to lyophilization.

Dynamic light scattering was used to obtain the basic characteristics of each fixed virus and NP type. An aliquot of the sample suspension (100 µL) was diluted into deionized water (900 µL) in a plastic cuvette and three measurements were taken to estimate the average diameter and size distribution using cumulants analysis with a Zetasizer- Nano-ZS (Malvern instruments; Southborough, UK). Sterile samples were stored in the freezer at -20^oC.

4.3.2 Clinical Trial

Twenty-five 1-day-old turkey poults (Aviagen, Lewisburg, WV) were raised in floor pens on pine shaving litter and provided feed and water ad libitum. At 6 weeks-of-age, when HEV maternal antibody had waned, they were randomly divided into five weight balanced groups of five birds each: unvaccinated (UN), empty particle (GC), nanovaccine (Nano), killed HEV with loose polymers (HP), and cell culture propagated live virus (LV) vaccine. The UN group was kept in a separate room within in the same building as the EP, Nano, and HP groups, which were kept in separate pens within the same room. The LV group was moved to a separate building and all health checks and treatments were given to this group last to avoid cross-contamination. Each group had the same pen dimensions (4 ft x 8 ft) and accoutrements throughout the study. The experimental vaccine treatments were reconstituted with distilled water as needed and administered using oral gavage. The unvaccinated group received no treatment and its data was removed from the subsequent results due to contamination. Serum was collected pre-vaccination at 6 weeks-of-age and then weekly for 3 additional weeks. The serum was frozen at t -20^oC prior to being used in the ProFLOK HEV Ab hemorrhagic enteritis virus antibody test kit (Zoetis, Parsippany-Troy Hills, NJ) .

All treatment groups were challenged with live HEV ($9.50E+04$ infectious virions as measured by qPCR). Birds were weighed and euthanized by CO2 displacement prior to necropsy at 5 days post-challenge to get the most accurate spleen weights. Spleen weights were obtained and samples from liver, kidney, and spleen

were taken for histopathology. Spleens were also frozen at -20^{o}C for subsequent qPCR analysis. As with the clinical study, the contaminated unvaccinated group was removed from analysis and therefore, the results and discussion sections will only include the twenty turkeys remaining. As there is no standardized grading criteria for enumerating germinal centers correlating to HEV infection, the pathologist after discussion with a poultry veterinarian chose to count the number of germinal centers in ten random 400x magnification fields per spleen.

4.3.3 Statistical Analysis

One-way ANOVA analysis was used to determine whether significant differences existed between sample groups and a student's t test was used to reveal which samples were significantly different. JMP Pro Software (v. 12.0.1, SAS Institute Inc., Cary, NC) was used for all statistical analysis. Data are reported as averages ± standard error with three replicates.

4.4 Results

The same fixation protocol optimized through design of experiment (DOE) and confirmed with real-time PCR (qPCR) as previously reported was used to kill the hemorrhagic enteritis virus (HEV). Briefly, HEV fixed with 0.02% paraformaldehyde for 6 hrs at 4°C was incubated with MDTC-RP19 lymphoblastoid cells (5E+05) for 8 days with a live virus control in order to confirm the fixed HEV was unable to replicate and thereby killed. Data are shown below in Table 4.1.

Table 4.1: qPCR results for fixation of HEV. Supernatant samples represent virus incubated with MDTC-RP19 turkey lymphoblastoid cells for 8 days (n = 3 wells per sample).

Virus Type	Number of Virions Detected)
Live HEV (starting amount)	$9.50E+04$
Live HEV (supernatant)	$2.13E+06$
Fixed HEV (supernatant)	$1.69E+03$

The fixed HEV was then characterized using dynamic light scattering (DLS) in different formulations: fixed HEV alone, HEV-GC nanovaccine, and HEV with polymers in addition to empty GC NPs. Data are shown below in Table 4.2.

Table 4.2: Average diameter and size distribution before and after purification of HEV, empty gelatin-chitosan (GC) NPs, hemorrhagic enteritis virus encapsulated in gelatin-chitosan (HEV-GC) nanovaccine, and HEV with polymers as measured using DLS. Each NP fabrication type was pelleted at 12,000 rpm for 5 mins, washed three times with PBS, resuspended in PBS, 0.22 filtered and lyophilized. Data are reported as average ± standard deviation (n = 3).

Nanoparticle Type	Average Diameter (nm)	Average Size Distribution
HEV	87.56±1.49	0.57±0.004
Empty GC NPs	250.99±24.63	0.33±0.061
HEV-GC Nanovaccine	261.08±27.50	0.32±0.080
HEV with polymers	74.64±9.27	0.53±0.049

An external laboratory measured the serum titers using a commercial HEV antibody test kit. Individual post-vaccination serum antibody titers are shown below in Figure 4.1.

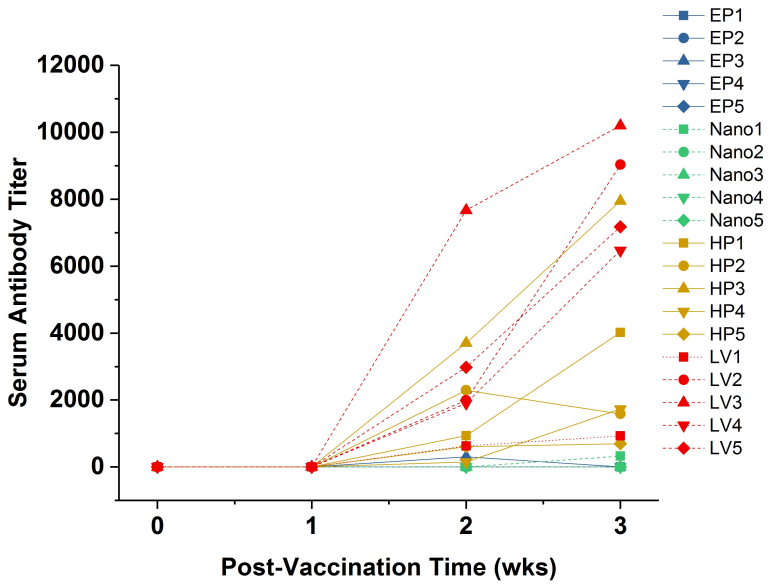

Figure 4.1: Post-vaccination serum antibody titers over time for EP, Nano, HP, and LV groups. Five turkeys per group.

The ratio of body weight to spleen weight at 5 days post challenge was calculated. The average results per treatment group are seen below in Figure 4.2.

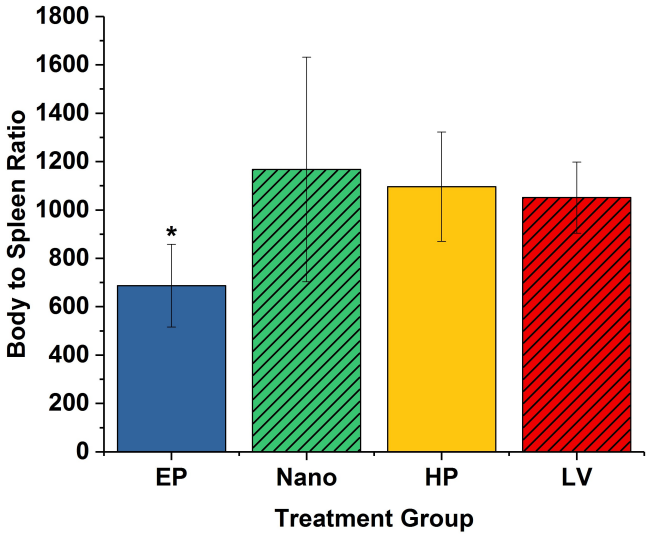

Figure 4.2: Body-to-spleen weight ratios for EP, Nano, HP, and LV groups. Five turkeys per group ($p \leq 0.05$)

To confirm the results from the body-to-spleen weights, qPCR was run on splenic samples to determine viral clearance. The average data per treatment group are shown below in Figure 4.3.

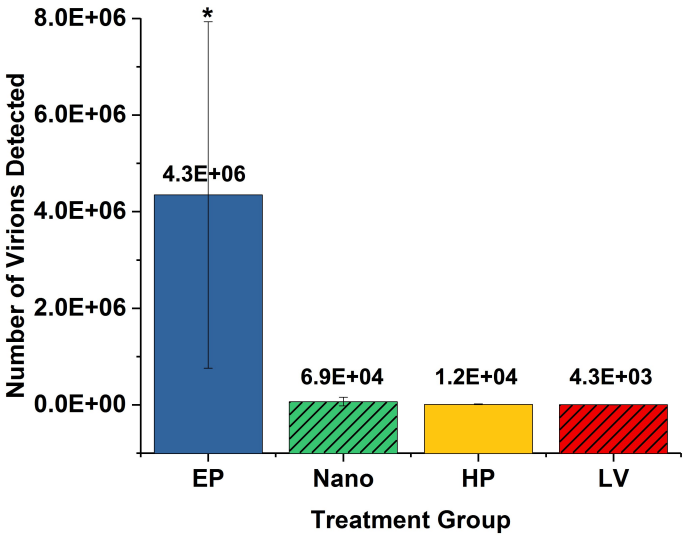

Figure 4.3: Splenic qPCR results for viral clearance. Group designations are as follows: EP, Nano, HP, and LV groups. Five turkeys per group. The genome copy number detected from the virions was significantly higher for the EP group compared to all other groups (n=3, $p < 0.05$)

A board certified blinded veterinary pathologist harvested the splenic samples during necropsy and analyzed them for histopathology. The turkeys and their respective samples were identified only through their wing band numbers to keep the pathologist blinded throughout the study. The number of germinal centers and intranuclear inclusions per ten fields (400x magnification, $2.37mm^2$) were manually counted for each splenic sample. These results are shown below in Table 4.3.

Table 4.3: Manual germinal center counts and intranuclear inclusions for empty nanoparticle (EP), nanovaccine (Nano), fixed HEV with polymers (HP), and live HEV (LV) treatment groups. Five turkeys per group.

Sample	Germinal Center Count	Intranuclear Inclusions Seen
EP1	1	+
EP2	1	+
EP3	0	+
EP4	0	+
EP5	1	+
Nano1	0	None
Nano2	0	None
Nano3	1	None
Nano4	1	None
Nano5	3	None
HP1	5	None
HP2	11	None
HP3	5	None
HP4	6	None
HP5	5	None
LV1	8	None
LV2	4	None
LV3	9	None
LV4	5	None
LV5	8	None

4.5 Discussion

A major hypothesis of this work was that a chemical fixative could kill HEV while still preserving the protruding siaylated fiber essential for its two-step cell entry mechanism [13,15]. Paraformaldehyde was chosen as the fixative chemical because of its well documented ability to kill viruses while preserving the protein ultrastructure [58, 54]. Prior to production of the clinical study treatments for the vaccine study, the paraformaldehyde fixation protocol's ability to kill HEV had to be validated. The same starting number of either live or fixed HEV virions as measured by qPCR genome copy number ($9.50E+04$) were incubated in MDTC-RP19 turkey lymphoblastoid cell culture for 8 days. Live HEV is able to replicate within the cell culture, leading to an increase in the number of infectious virions detected through qPCR genome copy number ($2.13E+06$) in Table 4.1 as compared to the genome copy number measured from the fixed HEV which did not increase ($1.69E+03$) over the same time frame. These results indicate the fixation protocol is able to prevent the HEV from replicating, which essentially renders the virus non-infectious or killed. Determination of whether the uptake mechanism remained intact was left for subsequent animal studies.

Once the HEV was shown to be killed, the next step was to create the vaccine treatment doses for the clinical study. Table 4.2 shows the average diameter and size distribution for each treatment and demonstrate the treatments were able to maintain a nanosize through purification and lyophilization. HEV as a biologic has a large size distribution (0.57), which is decreased with encapsulation in the nanoparticles (0.32). The HEV with polymers was included as a basic check for the treatment but having a mixture of polymer strands with the nanosize virus lead to less accurate DLS measurements.

In order to measure the ability of the different treatment formulations to induce protection, the following major results were gathered: individual serum antibody titers and average treatment group body-to-spleen weight ratios. In addition, two supportive analyses were used to confirm the findings from the major results: average treatment group splenic qPCR and individual splenic histopathology. In order the present the data as transparently and concisely as possible, a mix of individual results and average treatment group results have been shown.

The unvaccinated control group was removed from analysis of the clinical trial data due premature exposure to HEV (contamination) indicated by immunological profiles across results to the vaccinated groups. However, these birds were housed in a room separate from all other treatments. The EP group represented an additional HEV negative control and was co-housed with the Nano and HP groups. Challenge resulted in

infection of the EP group, indicating that these birds and the room as a whole were unlikely to have been prematurely infected as this would have resulted in protection form challenge. There was also no evidence of serconversion i.e., antibody against HEV-hexon, in either the EP or Nano groups prior to challenge.

In Figure 4.1, the individual post-vaccination serum antibody titers over three weeks were shown. This presentation of the data allowed individual antibody production to be seen over the full time period and captures the full response range of each treatment. None of the EP treatment group turkeys had significant measurable antibody response during the 3-week time period as expected. All the LV treatment group turkeys showed significant measurable antibody response and although the magnitude of the increase over time varied, four out of five achieved a serum antibody titer in the thousands by end of the 3 weeks. These two treatment groups represent the extremes of antibody production in response to a negative control treatment and a positive control treatment. Interestingly, the Nano treatment group also had minimal measurable antibody response similar to the EP group (negative control) while the HP group antibody production fell in between the extremes. Antibody production within three weeks post-vaccination is indicative of protective immunity for the current commercial live HEV vaccine [38]. Seroconversion of 60% or higher is considered indicative of full protection with splenic homogenate vaccine [24]. Extrapolating this benchmark to these results would suggest none of the EP group were protected (serum titer of 0 for each time point), only one bird in the Nano group was protected (one detectable serum titer result of 324 at week 3), all of the HP group were protected (all seropositive at week 2 through week 3) the LV group was completely protected (all seropositive at week 2 through week 3).

The seroconversion noted with the HP group may be due to accidental contamination through exposure to live virus although there is no evidence for contamination and the remaining results do not support contamination. A second hypothesis would be the killed virus electrostatically attached to the loose polymers, which then opened tight junctions and allowed the virus to move into the bloodstream and reach target cells. The virus' penton base and fiber could then facilitate uptake and internalization into the target cells. A third option is the polymers exerted their combined adjuvant effect through attracting antigen presenting cells to the themselves and increased the likelihood of the associated killed virus encountering its target cells for uptake. The fourth option is that the killed virus was taken up without any assistance from the polymeric adjuvants, which is unlikely but could be tested through addition of a killed virus control in a future study. A combination of these options may also explain the result.

The lack of antibody production seen with the Nano group may have multiple potential explanations. The

first is that the HEV-GC treatment truly did not stimulate the Th2 pathway to produce humoral immunity and therefore no antibodies were produced. The second is that antibodies were being produced but may have required a longer time frame to reach detectable levels in the blood using the ELISA method. The third is the ELISA used only detects antibodies against the HEV hexon and so if antibodies were produced against the fiber or penton base or another part of the virus, these would not be detected [83]. Humoral immunity is indicative of protection, but the gold standard is the body-to-spleen weight ratio[64, 25].

Because turkeys vary by breed in terms of weight and other physical characteristics, a comparison of the body-to-spleen ratios among the treatment groups is necessary to determine whether protective immunity has been achieved within any given study. The reasoning behind the ratio calculation is that live HEV will travel from the site of initial entry to the spleen and replicate there. In past studies, the degree of splenomegaly has been found to be proportional to viral dose as well as the most reliable measure of infection. Additionally, the body-to-spleen weight ratio is the most consistent parameter for measuring viral activity. There is evidence infection of macrophages and B cells in the spleen may lead to migration of additional macrophages and CD4+ T cells in the splenic white pulp, eventually resulting in white pulp hyperplasia and an increase in spleen weight[24, 64, 25]. To compensate for the fact that larger turkeys may start out with heavier spleens, the ratio of body weight to spleen weight is used. Turkeys without vaccine protection are expected to have heavier spleens due to infection and therefore, a lower body-to-spleen ratio as compared to turkeys with vaccine protection who should be able to clear the virus from the spleen more rapidly. Figure 4.2 shows that the EP group does indeed have a significantly lower average body-to-spleen ratio (687) in comparison to all other treatment groups. The Nano (1167), HP (1096), and LV (1051) treatment groups did not have significantly different body-to-spleen ratios from each other but all of these groups received a form of killed or live vaccine protection during the clinical study and prior to the live virus challenge, so it is expected they would be able to clear the virus and avoid significant inflammation.

Since the two major results were on a whole organism level, two additional supporting datasets were gathered on the DNA and tissue levels to confirm the previously discussed major results. The first supporting data was from splenic qPCR to measure viral clearance (Figure 4.3). This data was sought to support the body-to-spleen ratios as it was expected turkeys without vaccine protection would take longer to clear the virus from the spleen, leading to a higher number of measurable HEV DNA on the qPCR results. The hexon gene measure for this analysis has a one-to-one correlation with number of virions [52]. Here, we see the unprotected EP treatment group does indeed have a higher number of detectable virions (average $4.3E+06$)

in contrast to all other treatment groups. The Nano (average $6.9E+04$), HP ($1.2E+04$), and LV ($4.3E+03$) treatment groups were not significantly different from each other. This confirms the body-to-spleen ratio results that all the forms of killed or live vaccines given in the clinical study were able to protect their respective turkey treatment groups from the live HEV challenge.

The final piece of supportive data sought for this study was histopathology to look for differences in the number of splenic germinal centers and splenic intranuclear inclusions. Germinal centers are clusters of B lymphocytes and progenitors formed in response to vaccine stimulation to ultimately produce antibodies and long-term memory immune responses [4, 36]. HEV intranuclear inclusions are accumulations of viral protein within host cells that are characteristic of HEV infected cells. As there is not a standardized protocol for enumeration of germinal centers during HEV infection, the individual counts were included for transparency. The EP group having not seen the virus prior to the challenge study demonstrates the expected results for naive turkeys. In the 5-day period between live virus challenge and euthanasia, the EP treatment group turkeys' immune systems have not been able to mount a strong response to the virus leading to a lower number of splenic germinal centers despite the ongoing HEV infection. The entire EP treatment group also showed the typical adenoviral inclusions associated with HEV infection unlike all the other treatment groups. The adenoviral inclusions had typical lesions for HEV infection: moderate to marked reticuloendothelial hyperplasia with lymphoid depletion. That is to say, a characteristic cellular change in appearance was noted as commonly seen in HEV infection along with larger than normal numbers of phagocytic cells in the splenic tissue and a decrease in the immune cell tissue that mainly consists of lymphocytes. The Nano group also shows a low splenic germinal center count, which correlates with the lack of antibody production (Figure 4.1) as it appears the HEV nanovaccine was not able to stimulate humoral immunity through the B lymphocyte pathway although it did produce sufficient protective cellular immunity to clear virus from splenic tissue (Figures 4.2 and 4.3). By comparison, both the HP and the LV treatment groups showed higher numbers of germinal centers without adenoviral inclusions, suggesting both vaccine formulations were able to stimulate humoral immunity (Figure 4.1) and cellular immunity to clear the virus at the splenic level. These results are consistent with the antibody titers (Figure 4.1), body-to-spleen ratios (Figure 4.2), and qPCR splenic results (Figure 4.3).

4.6 Conclusions and Future Studies

Together, these results suggest the adjuvanted killed HEV vaccine formulations are safe, efficacious, and protective in the face of challenge. Paraformaldehyde was found to be sufficient to kill the virus without altering the virus to the extent of being unrecognizable to the target turkey immune cells for uptake, processing, and development of humoral and cellular immunity. The EP and LV treatment groups served as controls throughout both the clinical and challenge studies to provide benchmarks in the data for comparison to the Nano and HP treatment groups. The HEV-GC nanovaccine was able to protect the Nano treatment group turkeys from HEV infection on a cellular level but did not produce humoral immunity in contrast to the HEV with polymers treatment which was able to produce both types of immunity. This would suggest gelatin and chitosan are able to act as adjuvants in a vaccine formulation without being in nanoparticle form, eliminating the need for nanoparticle fabrication and simplifying the vaccine production process. Additionally, it is postulated chitosan is exerting its ability to open tight junctions, allowing the killed virus to more readily enter the bloodstream. This suggests chitosan does not need to be directly associated with the virus in nanoparticle form in order to act as an adjuvant. Future studies could include a more highly charged chitosan, such as trimethyl chitosan, which should improve chitosan's ability to open tight junctions and may better elucidate the mechanism behind its adjuvant effects. Additionally, an ELISA capable of detecting antibodies to different parts of the virus or an agar gel immunodiffusion test with whole virus would confirm whether humoral immunity was truly produced or not with the HEV-GC treatment. To confirm whether the HP and Nano formulations avoid the immunosuppression side effect of the live virus vaccination, a bacterial challenge study should be performed or at least a lymphocyte proliferation stimulation assay.

Both chitosan and gelatin adjuvants in loose polymer and nanoparticle formulations enabled the use of killed virus with an oral delivery vaccine. The loose polymer form is preferred due to simplifying the vaccine fabrication process and having more consistent results in producing more humoral and cellular immunity compared to the nanoparticle vaccine formulation. This development constitutes one of the first novel adjuvants discoveries in 70 years and opens the door for conversion of injectable vaccines to oral delivery, cross-species vaccine delivery, and drug delivery applications. This work contributes a new fixation method capable of killing virus while maintaining the body's ability to recognize and respond to whole virus antigen as well as two new oral polymer adjuvants to move the field of vaccine development forward toward next generation vaccines.

4.7 Acknowledgements

Authors would like to thank USDA NIFA Fellows Program (2018-67011-28039), VT Regenerative Medicine Interdisciplinary Graduate Education Program (IGEP), and the VT Biomedical Engineering and Mechanics Department for support; Dr. Patricia Dunn and the Pennsylvania Animal Diagnostic Laboratory System Penn State University (PADLS-PSU) for expertise with ELISA; Dr. Rami Dalloul for animal study expertise; and Dr. Nammalwar Sriranganathan and Dr. Thomas Cecere for lending their veterinary expertise.

Chapter 5

Conclusion

In this body of work, we sought to use an inert materials approach to demonstrate the feasibility of the double desolvation method for use with viral encapsulation, modify this method to minimize cytotoxicity in cell lines of interest, fabricate both FPV and HEV encapsulated NPs for use in cell studies to determine if uptake and cell growth could occur, and finally to test the HEV encapsulated NPs in clinical and challenge vaccine studies in turkeys. The results of the first two objectives found matching the encapsulation material size to empty NP size leads to preferred encapsulated NP formulation parameters and chitosan stabilizes NPs bypassing the need for cytotoxic crosslinkers. Paraformaldehyde was able to kill virus prior to vaccine formulation while still preserving virus morphology sufficiently for immune cell recognition. Both gelatin and chitosan were able to act as polymeric adjuvants in nanoparticle form and also in loose polymer form, stimulating protective immunity in an oral delivery vaccine. This development constitutes one of the first novel adjuvants discoveries in 70 years and opens the door for conversion of injectable vaccines to oral delivery across species.

Chapter 6

Acknowledgements

Author would like to acknowledge and thank the United States Department of Agriculture (USDA) National Institute of Food and Agriculture (NIFA) Agriculture and Food Research Initiative (AFRI), Biomedical Engineering and Mechanics Department, and Virginia Tech Regenerative Medicine Interdisciplinary Graduate Education Group (IGEP) for support; and Kathy Lowe at the Virginia Maryland College of Veterinary Medicine Morphology Lab and Stephen McCartney at the ICTAS Nanoscale Characterization and Fabrication Lab for help in SEM and TEM imaging. Many thanks to Nancy Tenpenny, Nammalwar Sriranganathan, Thomas Cecere, Rami Dalloul, Jerry Contreras, André Stevenson, Jr., Shelley Cooke, Hassan Mahsoub, Mark Van Dyke, Kevin Edgar, Yong Woo Lee, Abby R. Whittington, and Frank William Pierson for research support and advice.

Bibliography

[1] S.M. Ahsan and C.M. Rao. "The role of surface charge in the desolvation process of gelatin: implications in nanoparticle synthesis and modulation of drug release". In: *Int. J. Nanomed.* 12 (2017), pp. 795–808.

[2] C.L. Alfonso et al. "The genome of fowlpox virus". In: *J. Virol* 74 (2000), pp. 3815–3831.

[3] T.N. Alkie, R. Guenther, and S. Rautenschlein. "Molecular characterization of hemorrhagic enteritis viruses (HEV) detected in HEV-vaccinated flocks in Germany". In: *Avian. Dis.* 61 (2017), pp. 96–101.

[4] C.D.C. Allen, T. Okada, and J.G. Cyster. "Germinal Center Organization and Cellular Dynamics". In: *Immunity.* 27 (2007), pp. 190–202.

[5] Gelatin Manufacturers Institute of America. *Gelatin Handbook.* 2012.

[6] M. Amidi et al. "Chitosan-based delivery systems for protein therapeutics and antigens". In: *Adv. Drug. Deliv. Rev.* 62 (2010), pp. 59–82.

[7] E.D. del Amo and A. Urtti. "Current and future ophthalmic drug delivery systems a shift to the posterior segment". In: *Pharm. Sci. Technolog. Today.* 13 (2008), pp. 135–143.

[8] R. Ariyoshi et al. "Vaccination against Fowlpox Virus Via Drinking Water". In: *J. Vet. Med. Sci* 65 (2003), pp. 1127–1130.

[9] S. Azarmi et al. "Optimization of a two-step desolvation method for preparing gelatin nanoparticles and cell uptake studies in 143B osteosarcoma cancer cells". In: *J. Pharm. Pharm. Sci.* 9 (2006), pp. 124–132.

[10] G. Barhate et al. "*Quillaja saponaria* extract as mucosal adjuvant with chitosan functionalized gold nanoparticles for mucosal vaccine delivery: Stability and immunoefficiency studies". In: *Int. J. Pharm.* 441 (2013), pp. 636–642.

[11] B.C. Baudner et al. "Modulation of immune response to group c meningococcal conjugate vaccine given intranasally to mice together with LTK63 mucosal adjuvant and the trimethyl chitosan delivery system". In: *J. Infect. Dis.* 189 (2003), pp. 828–832.

[12] S. Bhatia. *Natural polymer drug delivery systems: nanoparticles, plants, and algae.* 1st. Switzerland: Springer International Publishing, 2016.

[13] U. Bilati, E. Allemann, and E. Doelker. "Nanoprecipitation versus emulsion-based techniques for the encapsulation of proteins into biodegradable nanoparticles and process-related stability issues". In: *AAPS PharmSciTech* 6 (2005), pp. 594–604.

[14] *Boehringer Ingelheim Vector vaccines.* 2017. URL: `http://avian.merial.com/vector-vaccines`.

[15] T.L Bowersock and S. Martin. "Vaccine delivery to animals". In: *Adv. Drug. Deliv. Rev.* 38 (1999), pp. 167–194.

[16] M. Brzoska et al. "Incorporation of biodegradable nanoparticles into human airway epithelium cells - in vitro study of the suitability as a vehicle for drug or gene delivery in pulmonary diseases". In: *Biochem. Biophys. Res. Commun.* 318 (2004), pp. 562–570.

[17] M. Bublot et al. “Development and use of fowlpox vectored vaccines for avian influenza”. In: *Amm. N.Y. Acad. Sci* 1081 (2006), pp. 193–201.

[18] A.E. Chambers, M.M. Dixon, and S.P. Harvey. “Studies of the Suitability of Fowlpox as a Decontamination and Thermal Stability Stimulant for Variola Major ”. In: *Int. J. Microbiol.* 2009 (2009), pp. 1–9.

[19] L. Chen and M. Subirade. “Chitosan beta-lactoglobulin core-shell nanoparticles as nutraceutical carriers”. In: *Biomaterials.* 26 (2005), pp. 6041–6053.

[20] C.J. Coester et al. “Gelatin nanoparticles by two step desolvation – a new preparation method, surface modifications and cell uptake”. In: *J. Microencapsul.* 17 (2000), pp. 187–193.

[21] S. Dash et al. “Kinetic modeling on drug release from controlled drug delivery systems”. In: *Acta. Pol. Pharm.* 67 (2010), pp. 217–223.

[22] A.J. Davison and B. Harrach. *Siadenovirus. In C. Tidona and G. Darai (eds) The Spring Index of Viruses*. 2011th ed. New York, NY: Springer, 2011.

[23] A.R. DeGroot and R.J. Neufeld. “Encapsulation of urease in alginate beads and protection from alpha-chymotrypsin with chitosan membranes”. In: *Enzyme. Microb. Technol.* 29 (2001), pp. 321–327.

[24] K. Dhama et al. “Haemorrhagic enteritis of turkeys - current knowledge”. In: *Vet. Quart.* 37 (2017), pp. 31–42.

[25] Avian Dis. “Role of splenectomy in prevention of hemorrhagic enteritis and death from hemorrhagic enteritis virus in turkeys”. In: 27 (1983), pp. 1106–1111.

[26] J.H. Eldridge et al. “Biodegradable microspheres: vaccine delivery system for oral immunization”. In: *Curr. Top. Microbiol. Immunol.* 146 (1989), pp. 59–66.

[27] A.O. Elzoghby. “Gelatin-based nanoparticles as drug and gene delivery system: reviewing three decades of research”. In: *J. Control. Release.* 172 (2013), pp. 1075–1091.

[28] A.O. Elzoghby, W.J. Samy, and N.A. Elgindy. “Protein-based nanocarriers as promising drug and gene delivery system”. In: *J. Control. Release.* 161 (2012), pp. 38–49.

[29] A.M. Fadly and K. Nazerian. “Efficacy and safety of a cell-culture live virus vaccine for hemorrhagic enteritis of turkeys: laboratory studies”. In: *Avian. Dis.* 28 (1984), pp. 183–196.

[30] O.C. Farokhzad and R. Langer. “Impact of Nanotechnology on Drug Delivery”. In: *ACS Nano.* 3 (2009), pp. 16–20.

[31] J. Francis. “Methods of infection and immunity in fowl pox”. In: *Aust. Vet. J.* 32 (1956), pp. 216–220.

[32] B. Gaihre et al. “Gelatin-coated magnetic iron oxide nanoparticles as carrier system: drug loading and in vitro drug release study”. In: *Int. J. Pharm.* 365 (2009), pp. 180–189.

[33] J. Garcia-Garcia et al. “Experimental studies and field trial with recombinant fowlpox vaccine in broilers in mexico”. In: *Avian. Dis.* 47 (2003), pp. 245–252.

[34] A.E. Gregory, R. Titball, and D. Williamson. “Vaccine delivery using nanoparticles”. In: *Front. Cell. Infect. Microbiol.* 3 (2013), pp. 1–13.

[35] R.K. Gupta, K. Rajesh, and G.R. Siber. “Adjuvants for human vaccines? current status, problems and future prospects”. In: *Vaccine* 13 (1995), pp. 1263–1276.

[36] E. Heinen et al. *In Vivo Immunology: Regulatory Processes during Lymphopoiesis and Immunopoiesis.* 1st. New York: Springer Science+Business Media, 1994, pp. 75–78.

[37] J.V. Van Den Hurk. “Propagation of group II avian adenoviruses in turkey and chicken leukocytes”. In: *Avian Dis.* 34 (1990), pp. 12–25.

[38] J.V. van den Hurk and S. van Drunen Littel-van den Hurk. “Chitosan nanoparticles as delivery systems for doxorubicin”. In: *Vaccine* 11 (1993), pp. 329–335.

[39] I. Jabbal-Gill et al. "Stimulation of mucosal and systemic antibody responses against Bordetella pertussis filamentous haemagglutinin and recombinant pertussis toxin after nasal administration with chitosan in mice". In: *Vaccine.* 16 (1998), pp. 2039–2046.

[40] M. Jahanshahi and Z. Babaei. "Protein nanoparticle: a unique system as drug delivery vehicles". In: *Afr. J. Biotechnol.* 194 (2008), pp. 4926–4934.

[41] K.A. Janes et al. "Chitosan nanoparticles as delivery systems for doxorubicin". In: *J. Control. Release.* 73 (2001), pp. 255–267.

[42] H.L. Jiang et al. "The potential of mannosylated chitosan microspheres to target macrophage mannose receptors in an adjuvant-delivery system for intranasal immunization". In: *Biomaterials.* 29 (2008), pp. 1931–1939.

[43] T. Jung et al. "Biodegradable nanoparticles for oral delivery of peptides: is there a role for polymers to affect mucosal uptake?" In: *Eur. J. Pharm. Biopharm.* 365 (2009), pp. 147–160.

[44] K. Khatri et al. "Plasmid DNA loaded chitosan nanoparticles for nasal mucosal immunization against hepatitis B". In: *Int. J. Pharm.* 354 (2008), pp. 235–241.

[45] E.R. Kovacs, M. Benki, and A. Erdei. *Adenoviruses: a comparative molecular and phylogenetic study.* 2011.

[46] A. Kumari, S.K. Yadav, and S.C. Yadav. "Biodegradable polymeric nanoparticles based drug delivery systems". In: *Colloids Surf. B.* 75 (2010), pp. 1–18.

[47] B. Lawson et al. "Emergence of a novel avian pox disease in British tit species". In: *PLOS ONE* 7 (2012), pp. 1–13.

[48] E. Leo et al. "Doxorubicin-loaded gelatin nanoparticles stabilized by glutaraldehyde: involvement of the drug in the cross-linking process". In: *Int. J. Pharm.* 155 (1997), pp. 75–82.

[49] H. Liang et al. "Genipin-crosslinked gelatin microspheres as a drug carrier for intramuscular administration: in vitro and in vivo studies". In: *J. Biomed. Mater. Res. Part A.* 65 (2003), pp. 271–282.

[50] I.M. van der Lubben et al. "Chitosan and its derivatives in mucosal and drug vaccine delivery". In: *Eur. J. Pharm. Sci.* 14 (2001), pp. 201–207.

[51] I.M. van der Lubben et al. "Chitosan for mucosal vaccination". In: *Adv. Drug. Deliv. Rev.* 52 (2001), pp. 139–144.

[52] H.M. Mahsoub et al. "Real-time PCR-based infectivity assay for the titration of turkey hemorrhagic enteritis virus, an adenovirus, in live vaccines ". In: *J. Virol Methods* 239 (2017), pp. 42–49.

[53] *Manual of Diagnostic Tests and Vaccines for Terrestrial Animals.* World Organisation for Animal Health, 2007, pp. 1–8.

[54] Y. Matsuda et al. "Comparison of fixation methods for preservation of morphology, RNAs, and proteins from paraffin-embedded human cancer cell-implanted mouse models ". In: *J. Histochem Cytochem* 59 (2011), pp. 68–75.

[55] J.B. McFerran and J.A. Smyth. "Avian adenovirus". In: *Avian. Dis.* 12 (2000), pp. 589–601.

[56] S.K. Mittal, A. Swaim, and Y.S. Ahi. *Adenoviral vectors: potential and challenges as a gene delivery system.* InTech, 2011.

[57] V.J. Mohanraj and Y.Chen. "Nanoparticles ? a review". In: *Trop. J. Pharm.* 5 (2006), pp. 561–573.

[58] L. Moller et al. "Evaluation of virus inactivation by formaldehyde to enhance biosafety of diagnostic electron microscopy". In: *Viruses* 7 (2015), pp. 666–679.

[59] S.R. Mudshinge et al. In: *Saudi. Pharm. J.* 46 (2011), 129–141, title = Nanoparticles: emerging carriers for drug delivery.

[60] E. Nagy et al. "Vaccination of 1-day-old chicks with fowlpox virus by the aerosol, drinking water, or cutaneous routes". In: *Avian. Dis.* 34 (1990), pp. 677–682.

[61] R. Nakaoka. "Potentiality of gelatin microsphere as immunological adjuvant". In: *Vaccine* 13 (1995), pp. 653–661.

[62] R. Narayani and K.P. Rao. "Preparation, characterization, and in vitro stability of hydrophilic gelatin microspheres using a gelatin-methotrexate conjugate". In: *Int. J. Pharm.* 95 (1993), pp. 85–91.

[63] T. Nochi et al. "Nanogel antigenic protein-delivery system for adjuvant-free intranasal vaccines". In: *Nat. Mater* 9 (2010), pp. 572–578.

[64] J.E. Ossa, R.C. Bates, and G.G. Schurig. "Hemorrhagic enteritis in turkeys: purification and quantification of the virus". In: *Avian Dis.* 27 (1983), pp. 235–245.

[65] L.J. Peek, C.R. Middaugh, and C. Berkland. "Nanotechnology in vaccine delivery". In: *Adv. Drug Deliv. Rev.* 60 (2008), pp. 915–928.

[66] N. Petrovsky and J.C. Aguilar. "Vaccine adjuvants: Current state and future trends". In: *Immunol. Cell. Biol.* 82 (2004), pp. 488–496.

[67] F.W. Pierson. "Current thoughts on the pathogenesis of hemorrhagic enteritis (HE), HE-associated secondary bacterial infections, diagnosis, control, and prevention". In: *11th ?Hafez? International Symposium on Turkey Diseases, World Veterinary Poultry Association* (2016).

[68] C. Porporatto, I.D. Bianco, and S.G. Correa. "Local and systemic activity of the polysaccharide chitosan at lymphoid tissues after oral administration". In: *J. Leukoc. Biol.* 78 (2005), pp. 62–69.

[69] F. Rauw et al. "The positive adjuvant effect of chitosan on antigen-specific cell-mediated immunity after chickens vaccination with live Newcastle disease vaccine". In: *Vet. Immunol. Immunopathol.* 134 (2010), pp. 249–258.

[70] S. Ravindranathan et al. "Effect of chitosan properties on immunoreactivity". In: *Mar. Drugs.* 14 (2016), pp. 1–12.

[71] C.P. Reis et al. "Nanoencapsulation I. methods for preparation of drug-loaded polymeric nanoparticles". In: *Nanomed-Nanotechnol.* 2 (2006), pp. 8–21.

[72] A. des Rieux et al. "Nanoparticles as potential oral delivery systems of proteins and vaccines: A mechanistic approach". In: *J. Control. Release.* 116 (2006), pp. 1–27.

[73] M. Roser, D. Fischer, and T. Kissel. "Surface-modified biodegradable albumin nano- and microspheres. II: effect of surface charges on in vitro phagocytosis and biodistribution in rats". In: *Eur. J. Pharm. Biopharm.* 19 (1998), pp. 225–263.

[74] S.K. Sahoo and V. Labhasetwar. "Nanotech approaches to drug delivery and imaging". In: *Drug. Discov. Today* 8 (2003), pp. 1112–1120.

[75] S.V. Sastry, J.R. Nyshadham, and J.A. Fix. "Recent technological advances in oral drug delivery - a review". In: *Pharm. Sci. Technolog. Today.* 3 (2000), pp. 138–145.

[76] Thermofisher Scientific. "A highly sensitive assay for endotoxin detection and quantitation for a variety of sample types". In: (2018).

[77] V. Shafer et al. "Phagocytosis of nanoparticles by human immunodeficiency virus (HIV)-infected macrophages: a possibility for antiviral drug targeting". In: *Pharm. Res.* 9 (1992), pp. 541–546.

[78] T.G. Shutava et al. "Layer-by-Layer-Coated Gelatin Nanoparticles as a Vehicle for Delivery of Natural Polyphenols". In: *ACS Nano* 3 (2009), pp. 1877–1885.

[79] M. Singh and D.T. Ohagan. "Recent advances in veterinary vaccine adjuvants". In: *Int. J. Parasitol. Parasites* 33 (2003), pp. 469–478.

[80] A.T. Stevenson et al. "The correlation between gelatin macroscale differences and nanoparticle properties: providing insight into biopolymer variability". In: *Nanoscale* 10 (2018), pp. 10094–10108.

[81] M.S. Sudheesh, S.P. Vyas, and D.V. Kohli. "Nanoparticle-based immunopotentiation via tetanus toxoid-loaded gelatin and aminated gelatin nanoparticles". In: *Drug. Deliv.* 18 (2011), pp. 320–330.

[82] Z. Sui et al. "Cross-protection against influenza virus infection by intranasal administration of M1-based vaccine with chitosan as an adjuvant". In: *Vaccine.* 28 (2010), pp. 7690–7698.

[83] D.E. Swayne. *Diseases of poultry.* 13th. Iowa: Wiley-Blackwell, 2013.

[84] *UMNSAH/DF-1.* 2019. URL: `https://www.atcc.org/Products/All/CRL-12203.aspx#culturemethod`.

[85] M. Villacres-Eriksson et al. "Involvement of interleukin-2 and interferon-gamma in the immune response induced by influenza virus iscoms". In: *Scand. J. Immunol.* 36 (1992), pp. 421–426.

[86] T. Villalobos. *Pfizer Animal Health In ovo technology.* 2017.

[87] J. Wang et al. "Evaluation of immune effects of fowlpox vaccine strains and field isolates". In: *Vet. Microbiol.* 116 (2006), pp. 106–119.

[88] C. Weber et al. "Desolvation process and surface characterization of protein nanoparticles". In: *Int. J. Pharm.* 194 (2000), pp. 91–102.

[89] G. Winzenburg et al. "Biodegradable polymers and their potential use in parenteral veterinary drug delivery systems". In: *Adv. Drug. Deliv. Rev.* 56 (2004), pp. 1453–1466.

[90] E. Wu et al. "Flexibility of the Adenovirus Fiber Is Required for Efficient Receptor Interaction". In: *J. Virol.* 77 (2003), pp. 7225–7235.

[91] R. Yadav and K. Balasubramanian. *Engineering of Nanobiomaterials: Application of Nanobiomaterials.* 1st. Oxford: Elsevier, 2016.

[92] K. Zhao et al. "Highly pathogenic fowlpox virus in cutaneously infected chickens". In: *Emerg. Infec. Dis.* 20 (2014), pp. 1200–1202.

[93] T. Zou et al. "Preparation, characterization, and induction of cell apoptosis of cocoa procyanidins-gelatin-chitosan nanoparticles". In: *Eur. J. Pharm. Biopharm.* 82 (2012), pp. 36–42.

[94] K. Zwiorek et al. "Delivery by cationic gelatin nanoparticles strongly increases the immunostimulatory effects of CpG oligonucleotides". In: *Pharm. Res.* 25 (2008), pp. 551–562.

Appendix A

A.1 Unvaccinated Treatment Group Clinical Trial Results and Rationale

An unvaccinated treatment group was included in the clinical trial. This group was housed with in the same building as the empty particle (EP), nanovaccine (Nano), and HEV with loose polymers (HP) groups but in a separate room and did not receive any treatment on day of inoculation. The group was removed from analysis due to evidence of contamination, which will be discussed here. The unvaccinated treatment group had no detectable antibodies over the three week period according to the T-HEV Assay. This suggests the unvaccinated group did not develop humoral immunity against HEV during the 3 weeks after the other groups were given treatments and is the expected result for an unvaccinated group.

Table A.1: Unvaccinated Treatment Group Body to Spleen Ratios

Group Member	Number of Detectable Virions
Unvacc1	600.67
Unvacc2	1152.99
Unvacc3	1414.14
Unvacc4	1450.78
Unvacc5	919.04

The Unvacc1 turkey had a low body-to-spleen ratio (600.67) as expected for unvaccinated birds and closely resembles the other negative control in the study, the EP group's data. The remaining four birds in the unvaccinated group had unexpectedly high body-to-spleen ratios and more closely resemble the Nano, HP, and LV groups. Overall, the average body-to-spleen ratio (1107.53) for the unvaccinated group suggested four turkeys in this group were contaminated with HEV and therefore had developed protective immunity against the live HEV challenge.

Table A.2: Unvaccinated Treatment Group Splenic qPCR Results

Group Member	Number of Detectable Virions
Unvacc1	$1.87E+06$
Unvacc2	$2.64E+02$
Unvacc3	$3.33E+03$
Unvacc4	$3.93E+03$
Unvacc5	$8.99E+02$

A similar trend to the body-to-spleen ratio unvaccinated group data was seen in the splenic qPCR results. Here, the Unvacc1 turkey had a large amount of detectable HEV DNA ($1.87E+06$) as expected for a naive turkey encountering the live HEV virus for the first time and prior to developing cellular immunity to quickly clear the virus from the spleen. The remaining four turkeys had low detectable amounts of HEV DNA and appear to have developed cellular immunity sufficient to clear the virus from the spleen. This supported the contamination initially found in the body-to-spleen ratios.

Table A.3: Unvaccinated Treatment Group Histopathology Results

Number of Germinal Centers	Intranuclear Inclusions
1	+
1	None
4	None
1	None
3	None

The histopathology results for the unvaccinated groups further supported the previous analyses and the overall conclusion of contamination. The germinal center count for the unvaccinated group was not as low as the other negative control EP group and falls in between that of the Nano and HP groups. This aligned with the lack of humoral immunity detected with serum antibody titers and suggested that perhaps humoral

immunity had progressed and might have been detectable at the time of euthanasia and necropsy. The intranuclear inclusions included suggested Unvacc1 had an active detectable HEV infection from the live HEV challenge as expected for a negative control. The remaining four birds had no intranuclear inclusions detected, which suggested the turkeys had developed cellular immunity sufficient to clear the virus without significant cell infection.

In conclusion, the Unvacc1 turkey had no humoral immunity based on serum antibody titer nor cellular immunity according to the body-to-spleen ratio, splenic qPCR results, and is likely actively infected based on the histopathology results. The other turkeys already had protective cellular immunity but no humoral immunity. The entire unvaccinated group should have resembled the EP group and the actively infected Uvacc1 turkey and was therefore contaminated. Of the remaining treatment groups, the live virus turkeys were kept in a separate building from all the other treatment groups to avoid contaminating the other groups with live virus.

While it appears some form of the virus contaminated four out of five birds in the unvaccinated treatment group, the EP, Nano, and HP groups were housed in a separate room within the same building as the unvaccinated group and these groups had no evidence of contamination. These three groups were housed in separate pens but within the same room and therefore shared bedding and airspace. Each of these groups has a different immunological profile across the data collected and if any turkey within this combined room became contaminated, all the turkeys within the combined room would have been infected with HEV within 5 days [83]. The strongest piece of evidence supporting the remaining groups were not contaminated is that the EP group, which was located in the middle pen between the Nano and HP groups, had a consistent immunological profile expected for a negative control naive to the virus across the humoral and cellular data gathered.

A.2 Vaccine Component Materials Characterization Results and Discussion

The Pierce^{TM} Chromogenic Endotoxin Quant KIt (Thermo Fisher Scientific; High Point, NC) was used to measure the endotoxin concentration in the polymeric vaccine components in order to check for contamination during the cell study phase and prior to use of these components in an *in vivo* study. Purified proteins passed

through high capacity endotoxin removal resins have endotoxin concentrations in the 1-5 EU/mL range, which is believed to correspond to 99% endotoxin removal [76]. Endotoxin contamination may be a major factor influencing the immunoreactivity of chitosan used in biomedical applications and was assessed in our experiments. Species differences appear to to influence endotoxin sensitivity and so these studies should be carried out in the cell lines and species of interest in order to get the most accurate results [70]. This data was gathered as a benchmark for future studies to show endotoxin contamination levels of gelatin and chitosan used in vaccine formulation within this range correlate with immunoreactivity without induction of overwhelming inflammation in turkeys. Future studies further characterizing these polymers will be needed in order to determine if the endotoxin contamination is causative of the immunoreactivity seen in the clinical trial.

Table A.4: Endotoxin Concentration in Vaccine Components

Vaccine Component	**Endotoxin Concentration (EU/mL)**
VB275 Gelatin	0.606
Chitosan	0.067
Chitosan (diluted 1:10)	0.036
GC NPs	0.998
HEV-GC NPs	1.021

The ThermoScientific 2,4,6- Trinitrobenzene Sulfonic Acid (TNBSA) Assay (Thermo Fisher Scientific; High Point, NC) was used to measure primary amine content in all three polymers used in this body of work. This data was gathered in order to gain a better understanding of the reactive amine groups available in each polymer. Molecular weight data has been previously described [80].

Table A.5: TNBSA Assay Results

Polymer Type	**Polymer Concentration (microgram/mL)**	**Amine Concentration (microgram/mL)**
SA300 Gelatin	210	2.02
VB275 Gelatin	190	2.34
Chitosan	0.036	190